



HAL
open science

4-Amino-1,2,4-triazole-3-thione-derived Schiff bases as metallo- β -lactamase inhibitors

Laurent Gavara, Laurent Seville, Filomena de Luca, Paola Mercuri, Carine Bebrone, Georges Feller, Alice Legru, Giulia Cerboni, Silvia Tanfoni, Damien Baud, et al.

► **To cite this version:**

Laurent Gavara, Laurent Seville, Filomena de Luca, Paola Mercuri, Carine Bebrone, et al.. 4-Amino-1,2,4-triazole-3-thione-derived Schiff bases as metallo- β -lactamase inhibitors. *European Journal of Medicinal Chemistry*, 2020, 208, pp.112720. 10.1016/j.ejmech.2020.112720 . hal-02997719

HAL Id: hal-02997719

<https://hal.science/hal-02997719>

Submitted on 10 Nov 2020

HAL is a multi-disciplinary open access archive for the deposit and dissemination of scientific research documents, whether they are published or not. The documents may come from teaching and research institutions in France or abroad, or from public or private research centers.

L'archive ouverte pluridisciplinaire **HAL**, est destinée au dépôt et à la diffusion de documents scientifiques de niveau recherche, publiés ou non, émanant des établissements d'enseignement et de recherche français ou étrangers, des laboratoires publics ou privés.

4-Amino-1,2,4-triazole-3-thione-derived Schiff bases as metallo- β -lactamase inhibitors

Laurent Gavara,^{a*} Laurent Seville,^{a,1} Filomena De Luca,^{b,2} Paola Mercuri,^c Carine Bebrone,^{c,3} Georges Feller,^d Alice Legru,^a Giulia Cerboni,^b Silvia Tanfoni,^b Damien Baud,^{a,4} Giuliano Cutolo,^{a,5} Benoît Bestgen,^{a,6} Giulia Chelini,^b Federica Verdirosa,^b Filomena Sannio,^b Cecilia Pozzi,^e Manuela Benvenuti,^e Karolina Kwapien,^{f,g,7} Marina Fischer,^h Katja Becker,^h Jean-Marie Frère,^c Stefano Mangani,^e Nohad Gresh,^f Dorothée Berthomieu,^g Moreno Galleni,^c Jean-Denis Docquier^{b*} and Jean-François Hernandez^{a*}

^a*Institut des Biomolécules Max Mousseron, UMR5247 CNRS, Université de Montpellier, ENSCM, Faculté de Pharmacie, 34093 Montpellier Cedex 5, France.* ^b*Dipartimento di Biotecnologie Mediche, Università di Siena, I-53100 Siena, Italy.* ^c*Laboratoire des Macromolécules Biologiques, Centre d'Ingénierie des Protéines-InBioS, Université de Liège, Institute of Chemistry B6a, Sart-Tilman, 4000 Liège, Belgium.* ^d*Laboratoire de Biochimie, Centre d'Ingénierie des Protéines-InBioS, Université de Liège, Allée du 6 août B6, Sart-Tilman, 4000 Liège, Belgium.* ^e*Dipartimento di Biotecnologie, Chimica e Farmacia, Università di Siena, I-53100 Siena, Italy.* ^f*Laboratoire de Chimie Théorique, UMR7616, Sorbonne Université, CNRS, 75252 Paris, France.* ^g*Institut Charles Gerhardt, UMR5253, CNRS, Université de Montpellier, ENSCM, 34296 Montpellier Cedex 5, France.* ^h*Chair of Biochemistry and Molecular Biology, Interdisciplinary Research Center, Justus Liebig University, D-35392 Giessen, Germany.*

¹⁻⁷Present address:

¹Institut Curie, Orsay, France.

²GSK Vaccines Institute for Global Health, Siena, Italy.

³Liège Université, GIGA, CHU B34, 11 avenue de l'Hôpital, 4000 Liège, Belgium.

⁴Selvita, Poznan, Poland.

⁵PrattLab, University of Southern California, Los Angeles, CA, USA.

⁶Medicines for Malaria Venture, Geneva, Switzerland.

⁷Sygnature Discovery, Nottingham, United Kingdom.

*Corresponding authors: Tel.: +33-(0)4 11 75 96 03; Fax: +33-(0)4 11 75 96 41.

E-mail addresses: jean-francois.hernandez@umontpellier.fr (J.-F. Hernandez); laurent.gavara@umontpellier.fr (L. Gavara); jddocquier@unisi.it (J.-D. Docquier).

Keywords: Metallo- β -Lactamase; 1,2,4-triazole-3-thione; Schiff bases; bacterial resistance; β -lactam antibiotic.

Abbreviations list

AMP, Ampicillin; *CAZ*, Ceftazidime; *CFX*, Cefoxitin; *COL*, Colistin; *DMSO*, dimethylsulfoxide; *DMEM*, Dulbecco's Modified Eagle Medium; *EDTA*, Ethylene diamine tetraacetic acid; *EGM*, Endothelial cell Growth Medium; *FCS*, Fetal Calf Serum; *HEPES*, 4-(2-Hydroxyethyl)-1-piperazine-ethanesulfonic acid; *hGloII*, human Glyoxalase II; *HUVEC*, Human Umbilical Vein Endothelial Cells; *IPM*, Imipenem; *ITC*, IsoThermal Calorimetry; *LC-MS*, liquid chromatography coupled to mass spectrometry; *LDH*, Lactate DeHydrogenase; *MBL*, metallo- β -lactamase; *MEM*, Meropenem; *MHB*, Mueller-Hinton broth; *MIC*, Minimum

Inhibitory Concentration; *MOPS*, 4-Morpholinopropane sulfonate; *MTT*, 3-(4,5-Dimethylthiazol-2-yl)-2,5-diphenyltetrazolium bromide; *TFA*, trifluoroacetic acid.

ABSTRACT

Resistance to β -lactam antibiotics in Gram-negatives producing metallo- β -lactamases (MBLs) represents a major medical threat and there is an extremely urgent need to develop clinically useful inhibitors. We previously reported the original binding mode of 5-substituted-4-amino/H-1,2,4-triazole-3-thione compounds in the catalytic site of an MBL. Moreover, we showed that, although moderately potent, they represented a promising basis for the development of broad-spectrum MBL inhibitors. Here, we synthesized and characterized a large number of 4-amino-1,2,4-triazole-3-thione-derived Schiff bases. Compared to the previous series, the presence of an aryl moiety at position 4 afforded an average 10-fold increase in potency. Among 90 synthetic compounds, more than half inhibited at least one of the six tested MBLs (L1, VIM-4, VIM-2, NDM-1, IMP-1, CphA) with K_i values in the μ M to sub- μ M range. Several were broad-spectrum inhibitors, also inhibiting the most clinically relevant VIM-2 and NDM-1. Active compounds generally contained halogenated, bicyclic aryl or phenolic moieties at position 5, and one substituent among *o*-benzoic, 2,4-dihydroxyphenyl, *p*-benzyloxyphenyl or 3-(*m*-benzoyl)-phenyl at position 4. The crystallographic structure of VIM-2 in complex with an inhibitor showed the expected binding between the triazole-thione moiety and the dinuclear centre and also revealed a network of interactions involving Phe61, Tyr67, Trp87 and the conserved Asn233. Microbiological analysis suggested that the potentiation activity of the compounds was limited by poor outer membrane penetration or efflux. This was supported by the ability of one compound to restore the susceptibility of an NDM-1-producing *E. coli* clinical strain toward several β -lactams in the presence only of a sub-inhibitory concentration of colistin, a permeabilizing agent. Finally, some compounds were tested against the structurally similar di-zinc human glyoxalase II and found weaker inhibitors of the latter enzyme, thus showing a promising selectivity towards MBLs.

1. Introduction

The development and spread of bacteria resistant to antibiotics is a very serious public health issue. The most relevant antibiotic resistance mechanism in Gram-negative opportunistic pathogens is the β -lactamase-mediated inactivation of β -lactam antibiotics, the most widely used group of antibacterial agents, which includes penicillins, cephalosporins and carbapenems [1-4].

β -Lactamases are grouped into four molecular classes: A, B, C, and D [5], showing an important heterogeneity of substrate profiles. Classes A, C and D are serine enzymes in which a serine residue plays a central role in the catalytic activity. Some of them (e.g. OXA-48- and KPC-type enzymes) also hydrolyse carbapenems, which are considered last resort antibiotics in the hospital setting. By contrast, all class B enzymes, which require a metal co-factor (one or two Zn ions(s)) for their activity, are all efficient carbapenemases, often characterized by an exceedingly broad substrate profile. These metallo- β -lactamases (MBLs) are classified into three subclasses: B1, B2, and B3, based on structural features [6]. The dizinc subclass B1 includes the most prevalent enzymes (e.g. VIM-, NDM-, and IMP-types) found in the clinical setting. However, whereas mono-zinc subclass B2 MBLs bear a limited clinical relevance, some subclass B3 di-zinc enzymes have also been recently acquired by relevant opportunistic pathogens (e.g. AIM-1, SMB-1). MBLs are produced by multi- to extremely drug-resistant clinical isolates belonging to some of the most clinically relevant Gram-negative bacterial species, causing a significant number of nosocomial infections (e.g. *Klebsiella pneumoniae*, *Enterobacter cloacae*, *Escherichia coli*, *Pseudomonas aeruginosa*, *Acinetobacter baumannii*). Furthermore, MBL-producing isolates, mainly found in the nosocomial setting, are also increasingly reported in isolates causing community-acquired infections [7]. Due to the global dissemination of carbapenem-resistant MBL-producing isolates, these enzymes are now regarded as major therapeutic targets, despite the discovery.

A validated approach to overcome β -lactamase-mediated resistance consists of combination therapy associating a β -lactam drug to a β -lactamase inhibitor, which protects the former from inactivation. Several β -lactamase inhibitors are currently available (clavulanate, tazobactam, sulbactam, avibactam, relebactam and vaborbactam), but they only target some serine- β -lactamases (SBLs) and are not active on MBLs [8]. In fact, the discovery and development of MBL inhibitors is extremely challenging. To our best knowledge, only one MBL inhibitor reached the stage of clinical development (taniborbactam or VNRX-5133, see below) [9-13], and there are only a few other lead compounds efficiently restoring bacterial sensitivity to

carbapenems [14,15]. Among the encountered difficulties, the subtle differences existing not only in the active sites of MBLs from the B1 and B3 subclasses but also within a same subclass render the discovery of a broad-spectrum inhibitor a true challenge [8,16]. Also, most published inhibitors possess a zinc-coordinating group, which represents a general approach for the inhibition of metallo-enzymes. Therefore, another difficulty is to avoid inhibition of some important human metallo-enzymes.

Numerous families of MBL inhibitors have already been described. The largest family of compounds possesses a thiol group [e.g. 17,18], which can be found in some marketed inhibitors of human metallo-peptidases (e.g. captopril, thiorphan). Whereas this group could afford highly potent inhibitors because of its strong Zn-binding properties, the consequence is a high risk for a lack of selectivity. Another important family of MBL inhibitors contains compounds with at least two carboxylate groups, such as succinate analogues [19], which were not further developed, or as aspergillomarasmine [20], a natural compound, whose inhibition mechanism at least partially resembles that of ethylenediaminetetraacetic acid (EDTA) [21]. Lack of selectivity could also be questioned for these compounds as, for instance, aspergillomarasmine was found to significantly inhibit ECE (Endothelin Converting Enzyme), an essential metallo-peptidase involved in blood pressure control [22]. Another Zn-chelating MBL inhibitor, Zn148, was also recently reported [23]. Finally, a more promising family is that of cyclic boronates, which are large spectrum inhibitors of both MBLs and SBLs (e.g. taniborbactam and QPX7728) [10-13,24,25]. Whereas extended studies revealed a favourable selectivity, the capacity of the boronate group to inhibit serine-, threonine- and metallo-hydrolases increases the number of potential off-target activities.

In this context, we are studying compounds containing a 1,2,4-triazole-3-thione moiety as an original zinc ligand. Otto Dideberg's group previously reported the 3D structure of L1, a di-zinc subclass B3 MBL, with a published inhibitor, XIII ([26] Figure 1) [27]. Surprisingly, the active site only contained a fragment (IIIA, Figure 1) produced via the hydrolysis of the hydrazone-like bond of XIII. Whether the enzyme itself catalyzed the hydrolysis remains to be determined. Furthermore, the inhibitor established an as yet unreported double coordination of the two Zn ions through two atoms of its 1,2,4-triazole-3-thione moiety (namely N² for Zn1 and S³ for Zn2). Starting from this observation, we undertook a large medicinal chemistry program to further assess the potential of these compounds as MBL inhibitors. We recently reported a first series of compounds, which were IIIA analogues (Figure 1) varying by their substituent at position 5 and substituted or not at position 4 by a NH₂ group [28]. In this series, quite modest

activities were obtained, but a few micromolar and broad-spectrum analogues (as tested against VIM-2, VIM-4, NDM-1, IMP-1, and L1) were identified, supporting the potential of this scaffold. In addition, we reported the X-ray structure of L1 in complex with the 4-H analogue of IIIA, which bound as IIIA but, unexpectedly, in a reverse manner [28]. *Ab initio* quantum chemical and polarizable molecular mechanics calculations of the complex formed by a triazole-thione motif with the dizinc active sites of L1 and VIM-2 have also been performed [29].

Meanwhile, it is noteworthy that, in addition to the original *in silico* screening by Olsen et al. on L1 [26], several other virtual and experimental library screenings, including fragment-based screening, on IMP-1 [30], VIM-2 [31] or NDM-1 [32] also identified this scaffold as a relevant di-zinc binding ligand. Furthermore, the resolution of the 3D structure of VIM-2 in complex with a small triazole-thione fragment showed a similar binding as IIIA in L1 [27,31]. These additional observations supported a very strong rationale for further investigation of these series. A special interest of the triazole-thione scaffold is that, compared to usual Zn ligands (e.g. thiol), it presents higher hindrance and lower flexibility because of the double coordination and is not as strong a Zn^{2+} ligand. This should offer a higher probability to spare human metallo-enzymes. Indeed, dizinc enzymes are much less abundant in humans than monozinc ones.

We herein report on a new series of 1,2,4-triazole-3-thione compounds based on Olsen's XIII Schiff base analogue [26] (Figure 1). Compared to IIIA analogues [28], the addition of an aryl moiety at the 4-position of the heterocycle led to more potent and broad-spectrum inhibitors of the most clinically relevant MBLs, including VIM-2, NDM-1 and IMP-1.

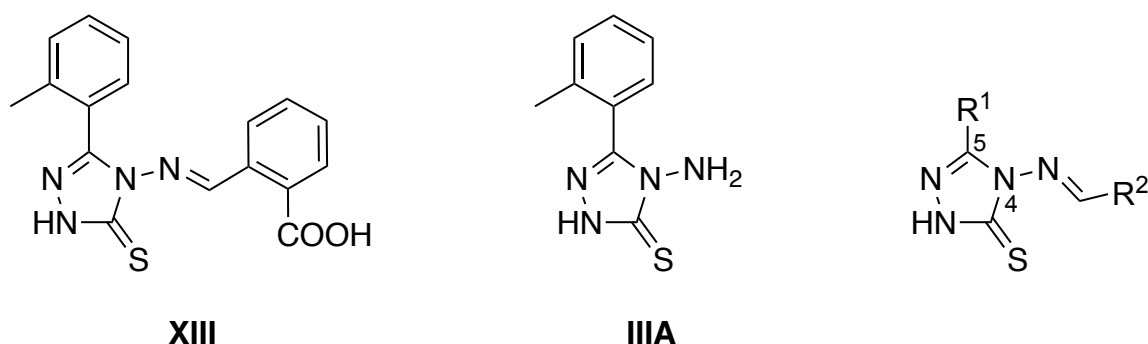
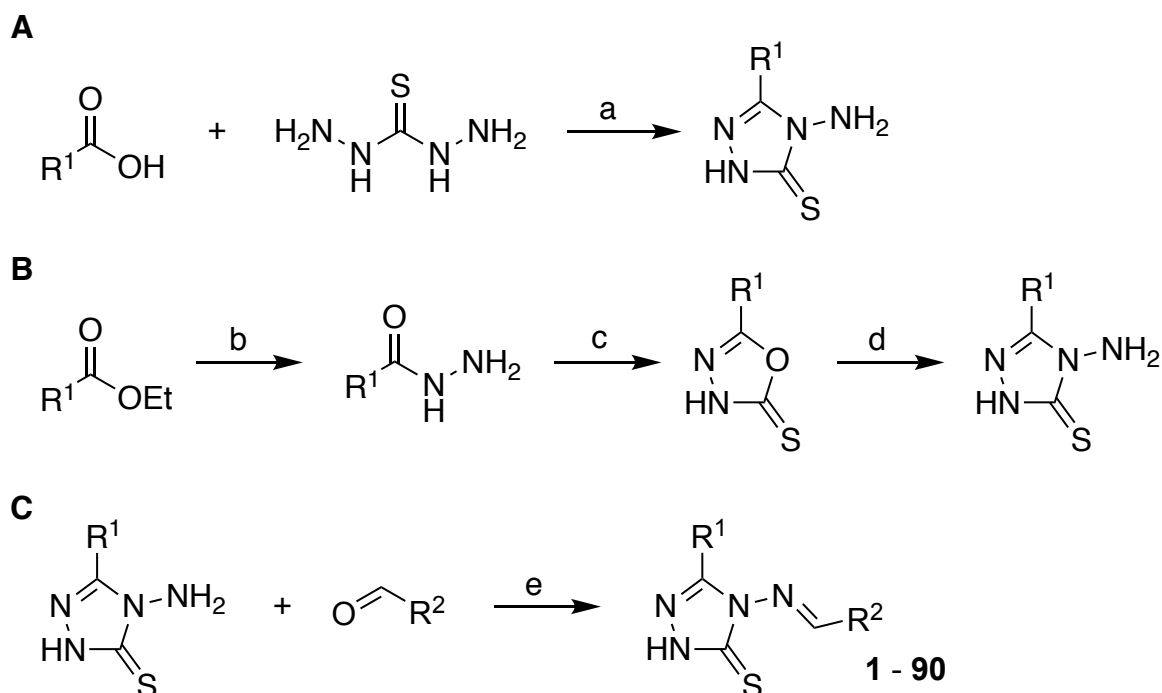


Figure 1. Structure of compound XIII (1), a 4-amino-1,2,4-triazole-3-thione-derived Schiff base [26], IIIA [27,28] and general structure of synthesized analogues.

2. Results and discussion

2.1. Synthesis



Scheme 1. Synthesis of 4-amino-1,2,4-triazole-3-thione derivatives. **A.** $R^1 \neq$ Aryl. **B.** $R^1 =$ aryl. **C.** Formation of Schiff bases **1-90** ($R^2 =$ aryl). Reagents and conditions: (a) neat, 160 °C; (b) hydrazine hydrate, neat, 120 °C, sealed tube; (c) CS_2 , KOH, EtOH, reflux; (d) hydrazine hydrate, EtOH, 100 °C, sealed tube; (e) AcOH, reflux.

The 4-amino-1,2,4-triazole-3-thione compounds, which bear the substituent at position 5, were synthesized as previously described [28]. Then, the substituent at position 4 was introduced by reaction between the 4-amino group and diverse benzaldehydes in the presence of acetic acid to yield Schiff bases **1-90**.

2.2. Evaluation of inhibitory potency toward purified MBLs

All compounds were tested against six representative MBLs, namely, the subclass B1 enzymes VIM-2, VIM-4, NDM-1 and IMP-1, the subclass B2 CphA and the subclass B3 L1. Some compounds were also tested against VIM-1. Initially, testing was performed at one concentration (100 or 200 μ M) and K_i values were measured for compounds exhibiting > 70% inhibition.

First, we found that compound XIII (**1**, Table 1) was indeed a more potent inhibitor than its heterocyclic fragment IIIA against all tested enzymes (for IIIA: $K_i = 108 \mu$ M (L1), 81 μ M (VIM-4), or $\leq 30\%$ inhibition at 100 μ M (VIM-2, NDM-1, IMP-1) [28]; no data for CphA). In

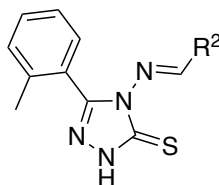
particular, XIII was a micromolar inhibitor of VIM-2 and VIM-4. In the case of L1 ($K_i = 40 \mu\text{M}$, a value in the same range as the IC_{50} ($15 \mu\text{M}$) reported by Olsen et al. [26]), the observed difference IIIA ($K_i = 108 \mu\text{M}$) suggested that XIII bound first to the enzyme, followed by Schiff base hydrolysis and accommodation of the IIIA fragment in the binding site as determined by crystallography [27]. It is not known if this scenario could be a general inhibition mechanism for all MBLs and XIII analogues.

Based on this result, we synthesized several series of 4-amino-1,2,4-triazole-3-thione-derived Schiff bases (XIII analogues). Their inhibitory potencies are listed in Tables 1, 2 and 3. Table 1 shows data obtained for XIII analogues where the substituent at position 4 was varied. The effect of variation at position 5 is presented on Table 2 and Table 3 shows the activities of compounds combining favourable 4- and 5-substituents.

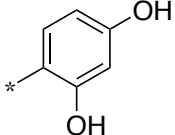
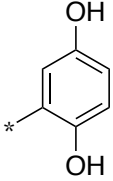
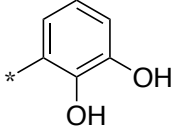
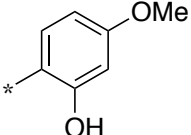
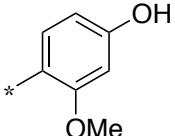
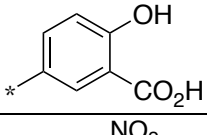
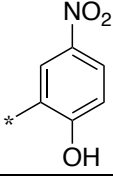
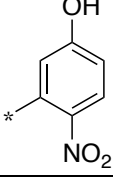
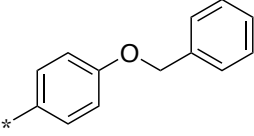
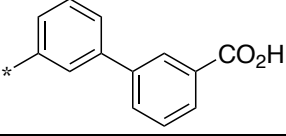
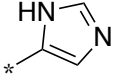
- Variation at position 4 (Table 1): the *o*-toluyl substituent at position 5 was kept unchanged and the *o*-benzoic moiety at position 4 was substituted with diverse aryl or heteroaryl groups. First, the absence of substituent on the aryl group (compound **2**) was deleterious to activity. All other compounds contained a mono- or di-substituted phenyl ring, with the exception of compound **21** that contained an imidazole ring.

In the case of compounds possessing an aryl mono-substituted by small chemical groups, replacement of the *ortho*-carboxylate group with a hydroxyl (**3**) or a nitrile (**5**) led to inactive compounds against all tested MBLs with the exception of VIM-2 and VIM-4, respectively. Similarly to compound **3**, compound **6** with an *o*-hydroxynapht-1-yl group was also inactive. In contrast, a nitro group at the *ortho* position (compound **4**) was more favourable as **4** not only possessed similar activities as compound XIII against L1, VIM-4 and NDM-1, but also higher potency against IMP-1 and particularly CphA (K_i , $5.0 \mu\text{M}$). With the exception of the 4-fluorinated analogue **7**, which was inactive against all tested MBLs, all other compounds with a small substituent at the *para* position showed micromolar K_i values against at least one MBL. Whereas **8** (*p*-CO₂H) moderately inhibited IMP-1, VIM-2 and CphA, **9** (*p*-OH) and **10** (*p*-NO₂) were potent inhibitors of VIM-4 with K_i values in the low micromolar range.

Table 1. Inhibitory activity of 4-amino-1,2,4-triazole-3-thione-derived Schiff bases **1-21** with R¹ = o-tolyl against various MBLs.



Cpd	Structure	<i>K_i</i> (μM) or (% inhibition at ^a 100 or ^b 200 μM)					
	R ²	L1	VIM-4	VIM-2	NDM-1	IMP-1	CphA
1		40.0	1.6	3.0	110	58.0	120
2		NI	20.0	20.0	(32%) ^a	(34%) ^a	70.0
3		NI	(38%) ^a	(62%) ^a	NI	(41%) ^a	NI
4		30.0	2.4	NI	NI	11.0	5.0
5		NI	6.5	NI	(60%) ^b	(50%) ^b	ND
6		NI	NI	NI	NI	NI	NI
7		(30%) ^a	NI	NI	(60%) ^b	(30%) ^a	ND
8		(59%) ^a	(57%) ^a	11.0	NI	11.0	31.0
9		(43%) ^a	1.3	NI	NI	(37%) ^a	(35%) ^a
10		(56%) ^a	1.4	NI	NI	(43%) ^a	(59%) ^a

11		31.0	0.4	7.0	NI	(45% at 50 μM)	62.0
12		(48%) ^a	1.6	11.0	(37%) ^a	(54%) ^a	(54%) ^a
13		(55%) ^a	(65%) ^a	5.2	(39% at 50 μM)	(63%) ^a	(68%) ^a
14		(55%) ^a	(55%) ^a	(58%) ^a	(32%) ^a	9.0	32.0
15		6.0	2.4	10.0	120	NI	4.0
16		13.0	1.4	2.0	120	(45%) ^a	(39%) ^a
17		(61%) ^a	(44%) ^a	NI	NI	11.0	3.0
18		16.0	(32%) ^a	NI	NI	(47%) ^a	9.0
19		12.0	2.1	NI	NI	0.3	22.0
20		0.9	0.3	1.10	NI	9.0	40.0
21		NI	NI	NI	NI	NI	(36%) ^a

NI: no inhibition (< 30% or < 50% inhibition at 100 or 200 μM, respectively). ND: not determined. ^a% inhibition at 100 μM; ^b% inhibition at 200 μM. Kinetics were monitored at 30 °C by following the absorbance variation observed upon substrate hydrolysis. *K_i*'s were determined when inhibition > 70% or for selected compounds showing broad-spectrum inhibition, regardless of their inhibition potency. Assays were performed in triplicate (S.D. ≤ 15%).

More significant results were obtained with compounds bearing disubstituted aryl moieties, which combined hydroxy, methoxy, carboxylic and nitro groups. The presence of two hydroxyl groups was favourable for inhibition of both VIM-4 and VIM-2. Among the three corresponding isomers **11**, **12** and **13** (respectively containing a 2,4-, 2,5- and 2,3-dihydroxyphenyl moiety), **11** with a hydroxyl group at the *para* position showed the best activity profile as it also moderately inhibited L1 and CphA. A *para*-hydroxyl group was also favourable in compounds **15** (methoxy group at the *ortho* position) and **16** (carboxyl group at the *meta*-position). In particular, **15** showed a large spectrum of activity with micromolar activities against four MBLs (i.e. L1, VIM-4, VIM-2, CphA) and measurable activity against NDM-1. In contrast, **14**, the reverse isomer of **15**, only showed significant activity against IMP-1. Finally, the two reverse isomers **17** and **18** (hydroxyl and nitro groups at the 2- and 5-positions) mainly showed significant inhibitory potency against CphA and were not or very poor inhibitors of VIM-type enzymes.

Attaching a second aryl group to the 4-aryl substituent yielded interesting compounds, **19** and **20**. Compound **19** with a *para*-benzyloxy moiety was a broad-spectrum inhibitor with significant activities against L1, VIM-4, IMP-1 and CphA. It is noteworthy that compound **19** was the best inhibitor of IMP-1 in this series with a K_i of 0.3 μM but was devoid of activity against VIM-2 and NDM-1. Compound **20** with a *meta*-benzoyl group at the 3-position of the 4-aryl substituent showed the largest spectrum in this series with micromolar to submicromolar potencies against L1, VIM-2, VIM-4 and IMP-1, while CphA was moderately inhibited.

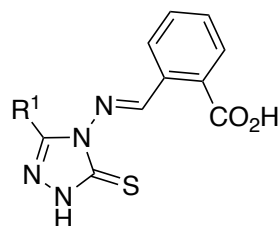
Finally, compound **21** bearing an imidazole substituent was found inactive toward all tested MBLs.

Overall, it is noteworthy that, although XIII was a modest inhibitor of NDM-1, none of these analogues were found to better inhibit this enzyme. In addition, among all substituents evaluated at position 4 of the triazole ring, some were of greater interest, including 2-carboxy-, 2,4-dihydroxy-, 4-benzyloxy-, and 3-(*m*-benzoic)-phenyl groups. Finally, a few compounds (i.e. **4**, **15**, **17**, **18**) inhibited the mono-zinc B2 enzyme CphA with K_i values in the micromolar range, confirming that this family of compounds could inhibit MBLs from all three sub-classes [28].

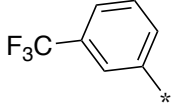
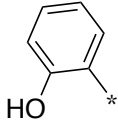
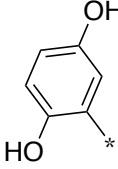
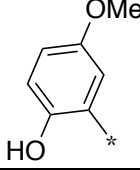
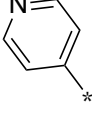
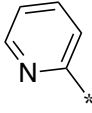
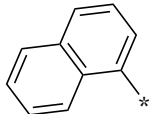
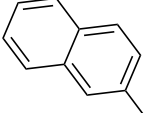
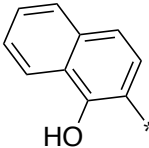
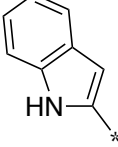
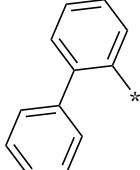
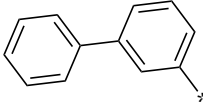
- Variation at position 5 of XIII (Table 2): the *o*-benzoic moiety at position 4 was kept unchanged and the *o*-toluyl substituent at position 5 was replaced by diverse aryl or heteroaryl groups directly attached to the triazole ring or through a one- or two-atom spacer.

Many substituents at position 5 in IIIA analogues (“short” series) were previously evaluated [28]. In these “short” series (i.e. only NH₂ or H at the 4-position), halogenated or bulky bicyclic aryl substituent at the 5-position were favourable for activity, whereas compounds containing more hydrophilic groups (i.e. phenol or heteroaryl) were less or not active. Overall, as observed for XIII (1) compared to IIIA, all Schiff bases were better inhibitors than their short counterparts. Furthermore, numerous compounds of this series showed better activity profile than XIII with larger spectrum and enhanced inhibitory potencies, including against NDM-1.

Table 2. Inhibitory activity of 4-amino-1,2,4-triazole-3-thione-derived Schiff bases **22-47** with R² = *o*-benzoic against various MBLs.



Cpd	Structure	<i>K_i</i> (μM) or (% inhibition at ^a 100 or ^b 200 μM)					
	R ¹	L1	VIM-4	VIM-2	NDM-1	IMP-1	CphA
1		40.0	1.6	3.0	110	58.0	120.0
22		5.0	1.4	2.7	38.0	NI	58.0
23		(60%) ^a	2.0	NI	7.5	58.0	ND
24		(60%) ^a	7.0	NI	7.6	NI	ND
25		3.0	0.8	3.0	30.0	(53%) ^a	4.0
26		3.0	2.0	(35%) ^a	NI	NI	ND
27		(40%) ^a	(51%) ^a	NI	NI	NI	ND

28		(40%) ^a	1.6	NI	3.2	(50%) ^b	(35%) ^a
29		(40%) ^a	3.0	2.2	NI	NI	ND
30		38.0	0.2	0.6	79.0	NI	52.0
31		9.0	0.5	0.7	27.0	NI	13.0
32		(32%) ^a	(73%) ^a	(50%) ^b	(50%) ^b	(45%) ^a	NI
33		NI	(62%) ^a	NI	(60%) ^b	NI	NI
34		1.1	(53%) ^a	14.5	76.0	(35%) ^a	(56%) ^a
35		4.62	0.4	0.7	2.3	10.6	NI
36		0.5	2.0	NI	(60%) ^b	NI	ND
37		(45%) ^a	NI	NI	9.4	54.7	ND
38		NI	(49%) ^a	NI	(32%) ^a	NI	ND
39		0.6	0.04	0.2	4.2	17.7	4.0

40		0.9	4.0	2.5	1.3	32.4	ND
41		0.4	1.0	0.9	2.8	(62%) ^a	ND
42		(59%) ^a	(57%) ^a	3.2	(60%) ^b	(48%) ^a	(51%) ^a
43		0.1	9.0	(50%) ^b	4.1	NI	13.0
44		0.5	5.0	2.4	1.7	34.4	15.0
45		4.0	(56%) ^a	7.0	NI	(37%) ^a	(50%) ^a
46		2.4	5.6	25.4	2.7	NI	15.0
47		(60%) ^a	3.0	2.0	2.4	(35%) ^a	(42%) ^a

NI: no inhibition (< 30% or < 50% inhibition at 100 or 200 μM , respectively). ND: not determined. ^a% inhibition at 100 μM ; ^b% inhibition at 200 μM . Kinetics were monitored at 30 $^{\circ}\text{C}$ by following the absorbance variation observed upon substrate hydrolysis. K_i 's were determined when inhibition > 70% or for selected compounds showing broad-spectrum inhibition, regardless of their inhibition potency. Assays were performed in triplicate (S.D. \leq 15%).

Simply removing the *o*-methyl group of XIII *o*-toluyl substituent yielded compound **22**, which not only exhibited similar micromolar inhibitory potency against VIM enzymes but also improved inhibition against L1, NDM-1 and CphA. Adding one halogen at the *meta* (Cl in **23**; Br in **26**; CF₃ in **28**) or *para* (Cl in **24**) position was well tolerated by VIM-4 but not by VIM-2 and L1 (with the exception of **26**). Interestingly, micromolar inhibitory potencies were measured against NDM-1 for the mono-chlorinated **23** and **24** and for the CF₃-bearing analogue

28 (K_i , 3.2 μM). The fluorinated compound **27** was poorly or not active on tested MBLs. Despite these mono-halogenated compounds possessed a restricted spectrum, the addition of a second chlorine substituent interestingly yielded the broad-spectrum inhibitor **25**. Indeed, this compound was a potent inhibitor of L1, VIM-2, VIM-4 and CphA, while showing some activity on NDM-1. The enhanced activity against NDM-1 that was observed in the halogen series is in agreement with the results obtained with the “short” counterparts of **23** and **28** [28].

In contrast to the corresponding “short” analogues, which were poorly or not active [28], the phenolic compounds **29-31** were potent inhibitors of VIM enzymes with submicromolar to micromolar K_i 's. In particular, **31** with a 2-hydroxy-5-methoxy-phenyl moiety exhibited a quite large spectrum (i.e. L1, VIM-2, VIM-4, CphA). However, while **30** and **31** moderately inhibited NDM-1, none was active against IMP-1.

Compared to their “short” analogues [28], which were completely inactive against all tested MBLs, the pyridine analogues **32** and **33** showed significant, although still modest, activities. In the “short” series, we reported that bi-aromatic substituents were highly favourable to MBL inhibition [28]. The same was true in the Schiff base series. Whereas compound **38** (*o*-biphenyl) was inactive and compounds **34** (naphth-1-yl), **36** (1-hydroxy-naphth-2-yl) and **37** (indol-2-yl) only potently inhibited one or two MBLs, all others exhibited a broad spectrum of activity with micromolar to submicromolar K_i 's: all MBLs for compound **39** (*m*-biphenyl); all but CphA for **35** (naphth-2-yl) and **40** (*p*-biphenyl, not tested against CphA); L1, VIM-4, VIM-2, NDM-1 for **41** (*p*-benzyloxyphenyl). In addition, some compounds could be tested on VIM-1 and **40** and **41** significantly inhibited this enzyme with K_i values of 7.1 and 3.9 μM , respectively.

We also synthesized analogues where the aryl substituent was separated from the triazole ring by one or two atoms. Whereas the benzyl (**42**) and phenethyl (**45**) derivatives only significantly inhibited one or two MBLs, all biaryl analogues (**43**, benzhydryl; **44**, naphth-2-ylmethyl; **46**, benzhydrylmethyl; **47**, naphth-2-yloxymethyl) exhibited a broad spectrum of activity, all with K_i values below 5 μM against NDM-1.

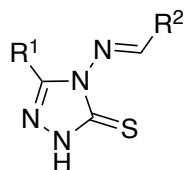
Therefore, by modifying the 5-substituent of XIII (**1**), we were able to increase the inhibitory potency against NDM-1, up to 80-fold for compound **40**, the best NDM-1 inhibitor reported in this paper (K_i , 1.3 μM). Although less important, an increase in potency was also observed against all other MBLs. Compared to other enzymes, IMP-1 was more sensitive to changes as most compounds were found inactive, but a few analogues were better IMP-1 inhibitors than XIII: the biphenyl analogues **39** and **40**, and the naphth-2-yl **35** and **44**. Overall, several compounds showed a broad spectrum of inhibition ($K_i < 10 \mu\text{M}$ toward several enzymes): in

particular, two compounds, **35** and **39**, showed K_i values in the submicromolar or low micromolar range against 5 out of 6 tested MBLs, which included two most clinically relevant MBLs NDM-1 and VIM-2. Compound **39** was also the best VIM-4 inhibitor reported in this paper (K_i , 40 nM).

- Combinations of substituents at positions 4 and 5 selected from the two preceding series (Table 3): selected substituents at position 5 (see Table 2) were combined with one, two, or all of the following 4-substituent(s) considered as the most favourable (see Table 1): 2,4-dihydroxyphenyl, *p*-benzyloxyphenyl and 3-(*m*-benzoic)-phenyl. We also synthesized the analogue without substituents on the two phenyl rings, **48**, which was inactive against all MBLs, except modestly so against IMP-1. Overall, removal of the carboxylate group on the 4-substituent phenyl was generally detrimental to activity. For instance, in the case of the most interesting broad-spectrum inhibitors possessing an *o*-benzoic group at position 4 (i.e. **22**, **25**, **35**, **39**, **40**, **43**, **44**, **46**, **47**, Table 2), its substitution led to a decrease in inhibitory potency against several if not all MBLs (respectively, **49**, **53**, [**67-69**], **74**, **77**, [**82**, **83**], [**84**, **85**], [**88**, **89**], **90**). The most drastic effect was observed with the analogues of the two best inhibitors from Table 2, **35** (naphth-2-yl in 5) and **44** (naphth-2-yl-methyl in 5): respectively, (i) **67** (2,4-dihydroxyphenyl in 4), **68** (*p*-benzyloxyphenyl in 4), **69** (3-(*m*-benzoic)-phenyl in 4), and (ii) **84** (2,4-dihydroxyphenyl in 4), **85** (*p*-benzyloxyphenyl in 4).

However, some interesting observations could be noted. The decrease in activity was mainly observed for L1 and VIM-2. In the case of L1, only two compounds exhibited K_i values below 10 μ M: **63** (2,4-dihydroxyphenyl in 5, 3-(*m*-benzoic)-phenyl in 4) and **65** (naphth-1-yl in 5, 2,4-dihydroxyphenyl in 4). Micromolar and submicromolar inhibitory potencies were measured against VIM-2 for only six compounds: five possessed a 2,4-dihydroxyphenyl substituent in 4 (i.e. **55**, **57**, **62**, **72**, **86**) and the fourth, a 3-(*m*-benzoic)-phenyl moiety (**63**). The corresponding parent analogues **11** and **20** (Table 1) also inhibited VIM-2 with a similar potency. All compounds containing a *p*-benzyloxyphenyl group in position 4 were inactive against this enzyme. This result confirmed that obtained for compound **19** (Table 1), suggesting that the VIM-2 binding site cannot accommodate this bulky substituent.

Table 3. Inhibitory activity of 4-amino-1,2,4-triazole-3-thione-derived Schiff bases **48-90** with combined R¹ and R² against various MBLs.



Cpd	Structure		<i>K_i</i> (μM) or (% inhibition at ^a 100 or ^b 200 μM)					
	R ¹	R ²	L1	VIM-4	VIM-2	NDM-1	IMP-1	CphA
48			NI	NI	NI	NI	(60%) ^a	NI
49			(46%) ^a	1.7	ND ^c	ND ^c	(54%) ^a	26.0
50			(60%) ^a	(35%) ^a	NI	6.7	NI	ND
51			(30%) ^a	3.0	(60%) ^b	(50%) ^b	(66%) ^a	(35%) ^a
52			(40%) ^a	NI	NI	4.1	NI	ND
53			(54%) ^a	(63%) ^a	(61% at 50 μM)	3.1	(67%) ^a	NI
54			18.0	0.6	NI	ND	0.1	NI
55			(40%) ^a	4.0	3.8	(50%) ^a	(55%) ^a	ND
56			(15%) ^a	NI	NI	NI	NI	ND
57			NI	13.0	0.62	(45%) ^a	NI	ND
58			NI	NI	NI	NI	(60%) ^a	ND
59			(25%) ^a	4.0	NI	11.7	NI	ND

60			NI	NI	NI	(50%) ^b	NI	ND
61			(15%) ^a	3.5	(53%) ^a	32.5	66.2	ND
62			(31%) ^a	0.5	2.0	NI	NI	6.0
63			2.7	0.09	0.13	NI	3.0	31.0
64			15.0	3.0	NI	NI	(50%) ^a	5.0
65			2.0	(32%) ^a	NI	NI	10.0	4.0
66			30.0	2.4	NI	NI	0.1	4.0
67			NI	(55%) ^a	NI	NI	NI	ND
68			NI	NI	NI	NI	NI	ND
69			(45%) ^a	2.8	(30%) ^a	(50%) ^b	NI	ND
70			NI	(55%) ^a	NI	NI	NI	ND
71			NI	NI	NI	NI	(60%) ^b	ND
72			NI	9.0	4.5	6.4	12.0	ND
73			NI	NI	NI	(45%) ^a	NI	ND
74			NI	(65%) ^a	(45%) ^a	(65%) ^a	NI	ND
75			NI	NI	NI	1.8	9.0	ND

76			NI	2.0	NI	1.8	NI	ND
77			NI	NI	NI	(64%) ^a	11.4	ND
78			NI	NI	NI	(42%) ^a	(62%) ^a	ND
79			NI	NI	NI	3.2	2.2	ND
80			(46%) ^a	(47%) ^a	(30%) ^a	NI	(37%) ^a	NI
81			(31%) ^a	NI	NI	NI	NI	5.5
82			NI	(50%) ^a	NI	NI	NI	ND
83			NI	NI	NI	(60%) ^b	(50%) ^b	ND
84			NI	(30%) ^a	NI	NI	(64%) ^a	ND
85			NI	NI	NI	NI	NI	ND
86			(51%) ^a	(54%) ^a	9.0	168	(45%) ^a	6.0
87			32.0	2.0	NI	(30%) ^a	9.0	1.0
88			(35%) ^a	NI	ND	ND	(35%) ^a	NI
89			NI	NI	NI	ND ^c	(30%) ^a	(30%) ^a
90			(40%) ^a	(60%) ^a	(30%) ^a	NI	(33%) ^a	NI

NI: no inhibition (< 30% or < 50% inhibition at 100 or 200 μ M, respectively). ND: not determined. ^a% inhibition at 100 μ M; ^b% inhibition at 200 μ M. ^cNot determined because of non-linear kinetics. Kinetics were monitored at 30 °C by following the absorbance variation observed upon substrate hydrolysis. K_i 's were determined when inhibition > 70%. Assays were performed in triplicate (S.D. \leq 15%).

By contrast, VIM-4 was more tolerant, as already noticed in the parent series (Tables 1 and 2). Indeed, fifteen compounds composed of 14 different 5-substituents and the three 4-substituents (2,4-dihydroxyphenyl: **49**, **51**, **55**, **57**, **59**, **61**, **62**, **64**, **72**, **76**; *p*-benzyloxyphenyl, **54**, **66**, **87**; 3-(*m*-benzoic)-phenyl: **63**, **69**) exhibited micromolar or submicromolar K_i values ranging 0.09 to 13 μM .

Although the parent XIII analogues containing a 2,4-dihydroxyphenyl (**11**) or a *p*-benzyloxyphenyl at position 4 (**19**) were inactive against NDM-1 (Table 1), eight compounds containing these two substituents potently inhibited this enzyme. This underlines the importance of the substituent at position 5, rather than at position 4, in providing better NDM-1 inhibitors. It is noteworthy that, with the exception of compound **72** (*o*-biphenyl in 5), all other compounds contained 5-aryl substituents, which were previously shown to be favourable (Table 2 and [28]), i.e. halogenated aryl (**50**, **52**, **53**, **59**) or biaryl ones (**75**, **76**, **79**). In contrast, although 5-arylalkyl-containing compounds with an *o*-benzoic group at position 4 (**43**, **44**, **46**, **47**) were potent NDM-1 inhibitors (Table 2), the related compounds **80-90** were inactive (Table 3).

Compared to compounds containing an *o*-benzoic group at the 4-position (Table 2), the results presented in Table 3 showed that, as already observed for compound **19** (K_i , 0.3 μM ; Table 1), a *p*-benzyloxyphenyl moiety at position 4 was highly favourable to IMP-1 inhibition, as K_i values ranging 0.1 to 11.4 μM were measured for compounds **54**, **66**, **75**, **77**, **79** and **87**. Three other molecules with either a 3-(*m*-benzoic)-phenyl (**63**) or a 2,4-dihydroxyphenyl moiety (**65**, **72**) also significantly inhibited this enzyme.

Finally, among 17 tested compounds, seven exhibited K_i values below 10 μM (i.e. **62**, **64-66**, **81**, **86**, **87**) against the subclass B2 enzyme CphA. All were better inhibitors than their related analogues with an *o*-benzoic group at the 4-position (**30**, **31**, **34**, **42**, **45**, Table 2).

Overall, whereas replacing the *o*-benzoic group at the 4-position was generally detrimental to inhibitory potencies and led to a narrower spectrum profile, a few compounds without this substituent nonetheless exhibited potent activity against at least one MBL. For instance, compounds **63** (K_i , 0.13 μM), **54** and **66** (K_i , 0.1 μM) and **87** (K_i , 1.0 μM) were respectively the best VIM-2, IMP-1 and CphA inhibitors reported in this paper. In addition, compounds **75** and **76** showed close K_i values (1.8 μM) to that of the best NDM-1 inhibitor **40**. Finally, this series afforded only two broad-spectrum inhibitors: (i) **63** with potent activities against L1, VIM-4, VIM-2 and IMP-1, but not NDM-1, as the related **20** (Table 1); (ii) **72**, which more moderately inhibited VIM-2, VIM-4, IMP-1, but also NDM-1.

- The thione group is essential to MBL inhibition: some compounds (**a-c**) where the sulphur atom was replaced by an oxygen (1,2,4-triazole-3-one scaffold) were synthesized and tested for inhibition (Scheme 1S and Table 1S). They shared the same 5-substituent (phenyl ring) and differed by their 4-substituent. **a** (*o*-benzoic), **b** (2,4-dihydroxyphenyl) and **c** (*p*-benzyloxyphenyl) were all inactive or only poorly active against both L1, VIM-4, VIM-2, NDM-1 and IMP-1 (Table 2S), confirming the crucial role of the sulphur in binding.

2.3. Isothermal calorimetry experiments (ITC)

The binding of selected compounds to VIM-2 was studied by ITC. Most inhibitors bound with an experimental stoichiometry n of 1.2-1.3, which clearly indicated a 1:1 association with the enzyme, consistent with X-ray crystallography data (see below). Accordingly, the compound concentration was lowered in the fitting procedure in order to provide $n \approx 1$ and to take account of compound solubility under ITC conditions. Typical ITC thermograms as well as data analyses by a Wiseman plot are shown for compound **63** in Figure 2 and compound **16** in Figure 1S.

The thermodynamic parameters of binding are given in Table 4 and are also depicted in Figure 3 for a more visual inspection (general explanations are provided in Supplementary Information). As shown, enthalpy drove the binding of most compounds (the enthalpic term is the major contributor to ΔG°_b and to affinity). Compounds **16**, **62**, and in particular **57** and **63** (the latter being among the best inhibitors of VIM-2 with K_i values of 0.62 and 0.13 μM , respectively) displayed the highest enthalpy values. Unfortunately, these favourable interactions were accompanied by a noticeable entropy penalty (tight binding and loss of freedom). Nevertheless, the favourable enthalpy contribution is an indication of specific interactions between binding partners and reflects ligand specificity and selectivity. Measured K_d values were close to K_i values (Tables 1 and 3). Interestingly, these four compounds did not contain an *o*-benzoic group at the 4-position in contrast to all other tested inhibitors, suggesting that this substituent was responsible of a specific behaviour.

In fact, all other investigated compounds (**22**, **25**, **31**, **35**, **39**) displayed a favourable entropic contribution, which was even the main contributor to affinity for the entropy-driven binding of compounds **22**, **25** and **35**. However, favourable interactions performed upon binding were relatively weak as reflected by the corresponding enthalpic contribution, and as a result, the affinity remained moderate. Overall, this suggested that favourable interactions occurring in the complex were replacing pre-existing bonds established with the solvent water and therefore the

net enthalpic effect was reduced due to desolvation [33,34]. In the case of these five compounds, K_d values were three- to five-fold lower than K_i values, with the exception of **35** for which these values were equal (Table 2).

Finally, the compounds displayed a nearly perfect enthalpy-entropy compensation phenomenon as illustrated in Figure 2S, which basically revealed that all compounds bound via the same molecular mechanism. The regression line with $r^2 = 0.98$ indicated that ITC experiments have retrieved high-quality data. The slope = 1.05 of this plot indicated that enthalpy (with favourable interactions) and entropy (tight binding or desolvation) equally contributed to the overall free energy of binding.

In the context of compound optimization, a strong preference is given to enthalpy-driven binding, with favourable entropic contribution (or at least a negligible contribution). In this respect, compound **39**, which not only displayed the highest affinity toward VIM-2 in this experiment but was also one of the two best broad-spectrum inhibitors in the present study, emerged as a promising candidate.

Table 4. Thermodynamic parameters of compounds binding to VIM-2 at 25 °C, listed by decreasing affinity.

Cpd (JMV)	n	K_a (M^{-1})	K_d (nM)	ΔG_b° (kcal/mol)	ΔH_b° (kcal/mol)	$T\Delta S_b^\circ$ (kcal/mol)
39	1.01 ± 0.01	1.5 ± 0.2 10 ⁷	68	-9.8	-7.2 ± 0.1	2.6
63	1.00 ± 0.01	7.2 ± 0.7 10 ⁶	139	-9.3	-13.7 ± 0.1	-4.4
57	1.03 ± 0.02	3.1 ± 0.6 10 ⁶	323	-8.8	-10.4 ± 0.2	-1.6
31	1.01 ± 0.01	2.6 ± 0.3 10 ⁶	389	-8.7	-6.3 ± 0.1	2.4
22	1.01 ± 0.03	1.9 ± 0.6 10 ⁶	519	-8.5	-3.6 ± 0.2	4.9
35	1.00 ± 0.01	1.4 ± 0.1 10 ⁶	713	-8.4	-3.3 ± 0.1	5.1
25	1.02 ± 0.01	1.2 ± 0.1 10 ⁶	863	-8.2	-3.9 ± 0.1	4.3
16	1.02 ± 0.01	7.7 ± 0.7 10 ⁵	1304	-8.0	-9.1 ± 0.2	-1.1
62	1.01 ± 0.04	3.4 ± 0.6 10 ⁵	2980	-7.5	-9.6 ± 0.5	-2.1

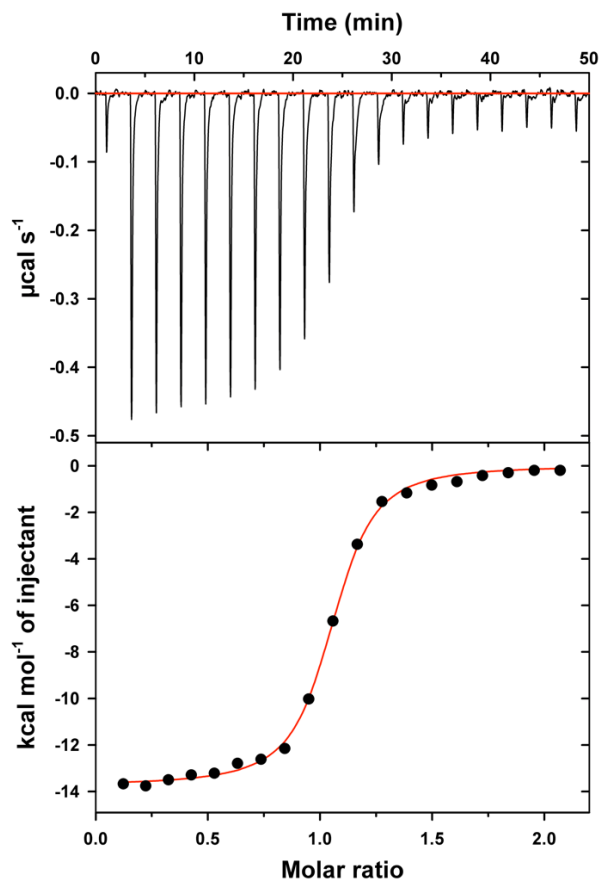


Figure 2. Isothermal titration calorimetry of VIM-2 by compound **63** at 25 °C. Upper panel: exothermic microcalorimetric trace of compound injections into VIM-2 solution (18.7 μM). Lower panel: Wiseman plot of heat releases versus molar ratio of injectant/protein in the cell and nonlinear fit of the binding isotherm for n equivalent binding sites. The binding enthalpy corresponds to the amplitude of the transition curve, K_a is derived from the slope of the transition and the stoichiometry n is determined at the transition midpoint.

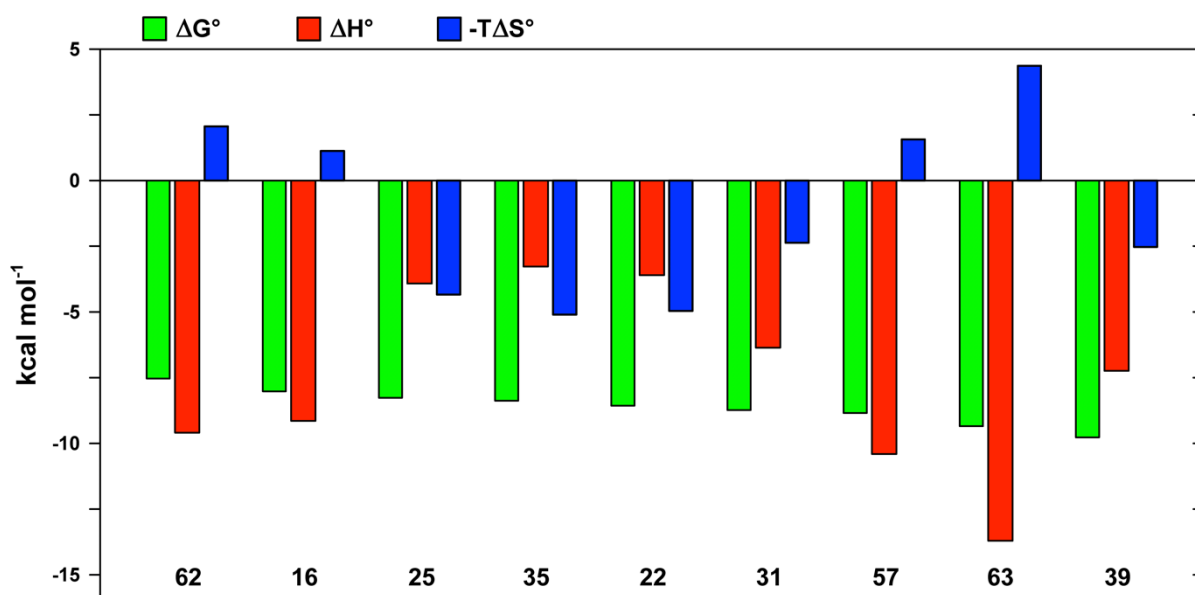


Figure 3. VIM-2 binding energetics of compounds, displayed by increasing affinity. Data are from Table 4 (see the general signification of thermodynamic signatures in Supporting Information).

2.4. *In vitro* antibacterial synergistic activity

The ability of selected compounds to potentiate the activity of β -lactam antibiotics was evaluated using several methods. First, a simple disk diffusion assay was performed on isogenic MBL-producing laboratory *Escherichia coli* strains, obtained by transforming strain XL-1 Blue or LZ2310 (a triple knock-out mutant of K12 in which genes encoding components of the major efflux pumps NorE, MdfA and AcrA were inactivated) with derivatives of the pLB-II plasmid in which the *bla*_{VIM-2}, *bla*_{VIM-4}, *bla*_{IMP-1}, and *bla*_{NDM-1} genes were cloned [35]. The latter strain was used to limit the potential efflux of the compounds, which would prevent sufficient accumulation in the periplasm. Compounds were tested according to their inhibition profile and availability. In this assay, some compounds were found able to significantly potentiate the activity of the antibiotic on LZ2310-derivative strains, mostly with the VIM-2-producing strain (Table 5). These include **1** and **22**, which interestingly restored susceptibility to the antibiotic (being above the EUCAST resistance breakpoint, 19 mm), as a diameter of the growth inhibition zone of 20 mm was measured. However, a more limited effect was observed when these compounds were tested on the wild-type strain XL-1 Blue, indicating that some inhibitors might behave as substrate of at least one of these efflux pumps. Nonetheless, compounds **13** and, to some extent, **61** provided some detectable potentiation of ceftiofloxacin on VIM-2-producing laboratory XL-1 Blue strain normally producing efflux pumps. Other compounds, despite being rather potent inhibitors, did not show any antibiotic potentiation, even when tested at up to 320 μ g and the efflux impaired strains, indicating that they might not be able to efficiently cross the outer membrane and accumulate in the periplasm at biologically relevant concentrations. This was especially true for compounds tested on the VIM-4- and NDM-1-producing strains. Compounds **17** and, to some extent, **29** showed potentiation when tested on the IMP-1-producing strain, with compound **17** showing a remarkable dose-dependent effect.

Table 5. *In vitro* synergistic activity of selected compounds measured by disk diffusion assays.

Cpd	Quantity (μ g) ^a	Diameter of growth inhibition zone (mm) observed with strains producing the following MBL ^b :				
		VIM-2	VIM-2 (XL-1) ^c	VIM-4	NDM-1	IMP-1
CFX ^d		14	8	-	-	-
AMP ^e		- ^g	-	6	-	-
CAZ ^f		-	-	-	15	9
1	40	17	-	-	-	-

	240	20	9	6	-	-
4	40	-	-	6	-	9
8	40	14	-	-	-	9
10	40	-	-	6	-	-
11	40	14	-	6	-	-
12	40	14	-	6	-	-
13	40	16	-	-	-	-
	80	18	15	-	-	-
14	40	-	-	-	-	9
15	40	14	-	7	-	-
16	40	14	-	6	-	-
17	40	-	-	-	-	13
	80	-	-	-	-	19
19	40	-	-	6	-	9
20	40	14	-	6	-	9
22	40	20	-	-	-	-
23	320	14	8	-	15	9
24	80	-	-	-	15	-
25	40	14	-	6	-	-
28	40	-	-	-	15	-
29	320	17	10	-	-	12
30	40	14	-	6	-	-
31	40	14	-	6	-	-
35	40	15	-	-	15	9
37	40	14	-	-	15	9
39	320	15	9	-	-	9
40	80	15	-	-	16	-
41	40	14	-	-	15	-
42	40	14	-	-	-	-
43	40	14	-	-	15	9
44	40	14	-	-	15	9

	120	16	-	-	-	-
45	40	14	-	-	-	-
46	40	14	-	-	15	-
47	40	14	-	-	15	-
49	40	-	-	6	-	-
50	40	-	-	-	15	-
52	40	-	-	-	15	-
53	40	-	-	-	15	-
54	40	-	-	6	-	9
55	40	14	-	-	-	-
59	40	-	-	-	15	-
61	120	-	12	-	-	-
62	40	14	-	6	-	-
63	40	14	-	6	-	9
65	40	-	-	-	-	10
66	40	-	-	6	-	9
71	80	-	-	-	-	9
72	80	14	-	-	15	-
75	80	-	-	-	15	-
76	80	14	-	-	15	-
77	320	16	10	-	-	11
79	80	-	-	-	15	-
85	80	-	-	-	-	9
86	40	14	-	-	-	-
87	40	-	-	6	-	9
89	40	-	-	-	15	-

^aQuantity of compound, dissolved in DMSO, deposited on the antibiotic-containing disks. DMSO was used as a control and did not affect the diameter of the growth inhibition zone. 220 µg EDTA were used as inhibition control and restored full susceptibility to the antibiotic. ^bMBL-producing strains were obtained by transforming the pLB-II plasmid carrying the cloned MBL gene in strain LZ2310 (triple knock-out mutant of efflux pumps), unless otherwise specified. ^cStrain obtained by transforming *E. coli* XL-1 Blue with the pLBII-VIM-2 plasmid, and used to assess the potential activity of the compound in a wild type strain, i.e. in which the efflux pumps are normally produced. ^d30 µg cefoxitin (CFX) disks were used to test VIM-2 producing strains. ^e10 µg ampicillin (AMP) disks were used to test the VIM-4-producing strain. ^f30 µg ceftazidime (CAZ) disks were used to test NDM-1- and IMP-1-producing strains. ^gNot determined.

Furthermore, and considering the growing epidemiological relevance of NDM-type carbapenemases, compounds showing K_i values lower than 2 μM on NDM-1 (compounds **40**, **44**, **75**, **76**) were also evaluated for their potential activity on a NDM-1-producing multidrug-resistant clinical isolate, which also produces other β -lactamases, including the extended-spectrum β -lactamase CTX-M-15, using a broth microdilution method. Tested at a fixed concentration of 32 $\mu\text{g}/\text{mL}$, these compounds showed some effect, although limited, with carbapenems (up to 4-fold reduction of the MIC value for **76**) (Table 6). Ceftazidime MIC was not affected by any MBL inhibitors likely due to the production of class A extended-spectrum β -lactamase. In the presence of avibactam, a potent inhibitor of serine- β -lactamases, resistance to ceftazidime (and thus to ceftazidime-avibactam) relies on the production of the NDM-1 enzyme. Compound **76** proved slightly more effective when the medium was supplemented with a sub-inhibitory concentration of colistin (that did not affect MIC values on its own), a polymyxin antibiotic well known for its membrane permeabilizing properties [36]. In these conditions, carbapenem MIC values were further reduced by a 2-fold factor. The effect of colistin was especially remarkable (64-fold reduction of the MIC value) with ceftazidime-avibactam, as the addition of both **76** and colistin was able to restore full susceptibility to the combination.

Table 6. Antibacterial activity of various β -lactam antibiotics in the absence and presence of selected compounds on a NDM-1-producing *E. coli* clinical isolate determined by the broth microdilution method.

Cpd (32 $\mu\text{g}/\text{mL}$)	MIC ^a ($\mu\text{g}/\text{mL}$) for <i>E. coli</i> ($bla_{\text{NDM-1}}^+$)			
	IPM	MEM	CAZ	ZAV
None	16	64	>256	>256
40	8	32	>256	>256
44	8	64	>256	>256
75	8	64	>256	>256
76	8	16	>256	>256
76 + 0.12 $\mu\text{g}/\text{mL}$ COL ^b	4	8	>256	4

^aIPM, imipenem; MEM, meropenem; CAZ, ceftazidime; ZAV, ceftazidime/avibactam (avibactam was tested at a fixed concentration of 4 $\mu\text{g}/\text{mL}$); ^bTested in the presence of sub-inhibitory concentration of colistin (COL).

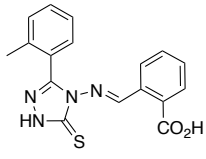
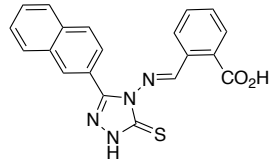
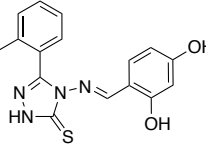
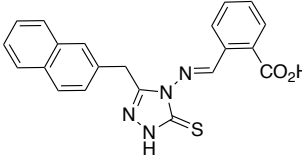
Altogether, these experiments (disk diffusion assays with wild-type and efflux-impaired strains and broth microdilution assays, including with colistin) indicated that the accumulation of these inhibitors in the bacterial periplasm might rely on both efflux mechanisms and limited diffusion through the outer membrane, explaining their limited activity in whole cell assays, despite the submicromolar inhibitory activity observed on purified enzymes.

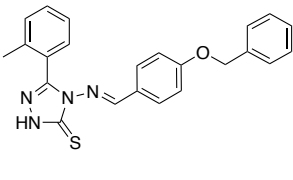
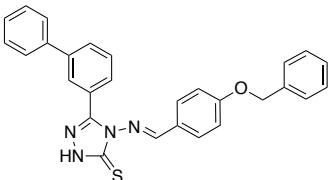
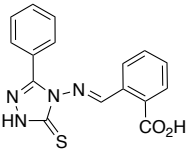
However, the encouraging potentiation effect of compound **76** with both meropenem and ceftazidime-avibactam (in the presence of colistin) supports the potential of these compounds as a starting point of further medicinal chemistry efforts to overcome current limitations.

2.5. Selectivity toward human glyoxalase II

A representative panel of compounds (**1**, **11**, **19**, **22**, **35**, **44**, **75**) was tested against human glyoxalase II, a bi-zinc metallo-hydrolase belonging to the MBL superfamily. Table 7 shows that all compounds could inhibit human glyoxalase II with IC₅₀ values between 5.9 μM (**19**) and 30 μM (**44**). Unfortunately, in spite of several approaches, exact K_i could not be determined for the human enzyme. However, although K_i and IC₅₀ values can only be indirectly compared, most tested compounds were found more potent inhibitors of some MBLs. In particular, the broad-spectrum MBL inhibitors **35** and **44** showed clear selectivity in favour of VIM-2, VIM-4, NDM-1 and L1.

Table 7. Inhibitory activities of compounds against human glyoxalase II.^a

Cpd	Structure	IC ₅₀ (μM)	Cpd	Structure	IC ₅₀ (μM)
1		25.8	35		13.2
11		19.0	44		30.0

19		5.9	75		23.4
22		25.5			

^aGloII activity was measured by following the decrease in absorbance at $\lambda = 240$ nm. All experiments were carried out in duplicate. Results are provided as mean values that differed by less than 15%.

2.6. Cytotoxicity assays on mammalian cells

The potential cytotoxicity of compound XIII (**1**) was assessed against HUVEC (human umbilical vein endothelial cells) using the MTT assay. No toxicity was observed up to 100 μ M concentration (Figure 3S). Furthermore, compound **76** did not induce cell lysis using a membrane integrity assay (HeLa cells) at concentrations up to 250 μ M. This result was also confirmed using a cell viability assay (HeLa cells, 1,500 cells/well), in which no cytotoxic effects could be observed after up to 72h of incubation in the presence of 250 μ M **76**.

2.7. Crystal structure of the VIM-2/cpd **31** complex

The three-dimensional structure of VIM-2 inhibited by compound **31**, one of the most potent VIM-2 inhibitor described herein, was obtained at 1.95 Å resolution (Figure 4, PDB code, 6YRP). The binding of the inhibitor did not alter the tertiary structure of the enzyme (RMSD, 0.176 Å: 210 C α atoms). The structure showed that the triazole-thione moiety similarly established a simultaneous double coordination of the active site zincs, displacing the catalytic hydroxide ion, as previously reported for short triazole-thione compounds in the active site of L1 [27] (Figure 4D) or VIM-2 [31], the nitrogen at position 2 coordinating Zn1, while Zn2 was interacting with the inhibitor sulphur atom. However, in contrast to what was observed in the study by Nauton et al. [27] (i.e. IIIA, a hydrolysis-derived fragment of XIII (**1**), was present in the L1 active site), the entire Schiff base **31** was clearly present in the VIM-2 active site (as revealed by the electron density map, Figure 4B), showing that hydrolysis of the hydrazone-like bond did not occur in this case. Compound **31** interacted with several active site residues (Figure 4C). In particular, the methoxy and hydroxy oxygen atoms of the substituent at position 5 were H-bonded to the NH of Trp87 and NH₂ of the conserved Asn233, respectively.

Surprisingly, the carboxylate moiety did not interact with Arg228 but was rather H-bonded to the backbone NH of Asn233 and further interacted with two water molecules. Another water molecule was found to form an H-bond with the N1 atom of the triazole ring. The side-chain of Arg228 was slightly displaced outwards the active site to accommodate the inhibitor. Finally, the aromatic rings also interacted with the side chains of Phe61 and Tyr67 with the establishment of T-shaped π stacking interactions and, for the benzoate moiety, with the conserved His263 residue through parallel π stacking interactions.

Therefore, compound **31** interacted with several conserved residues in the active site, including the catalytically important Asn233, His263 and the hydrophobic residues Phe61, Tyr67 and Trp87 (the latter also present in NDM-1), located in loop L1 and defining one side of the active cavity. Overall, this structural information provides a structural basis to drive the synthesis of further compounds.

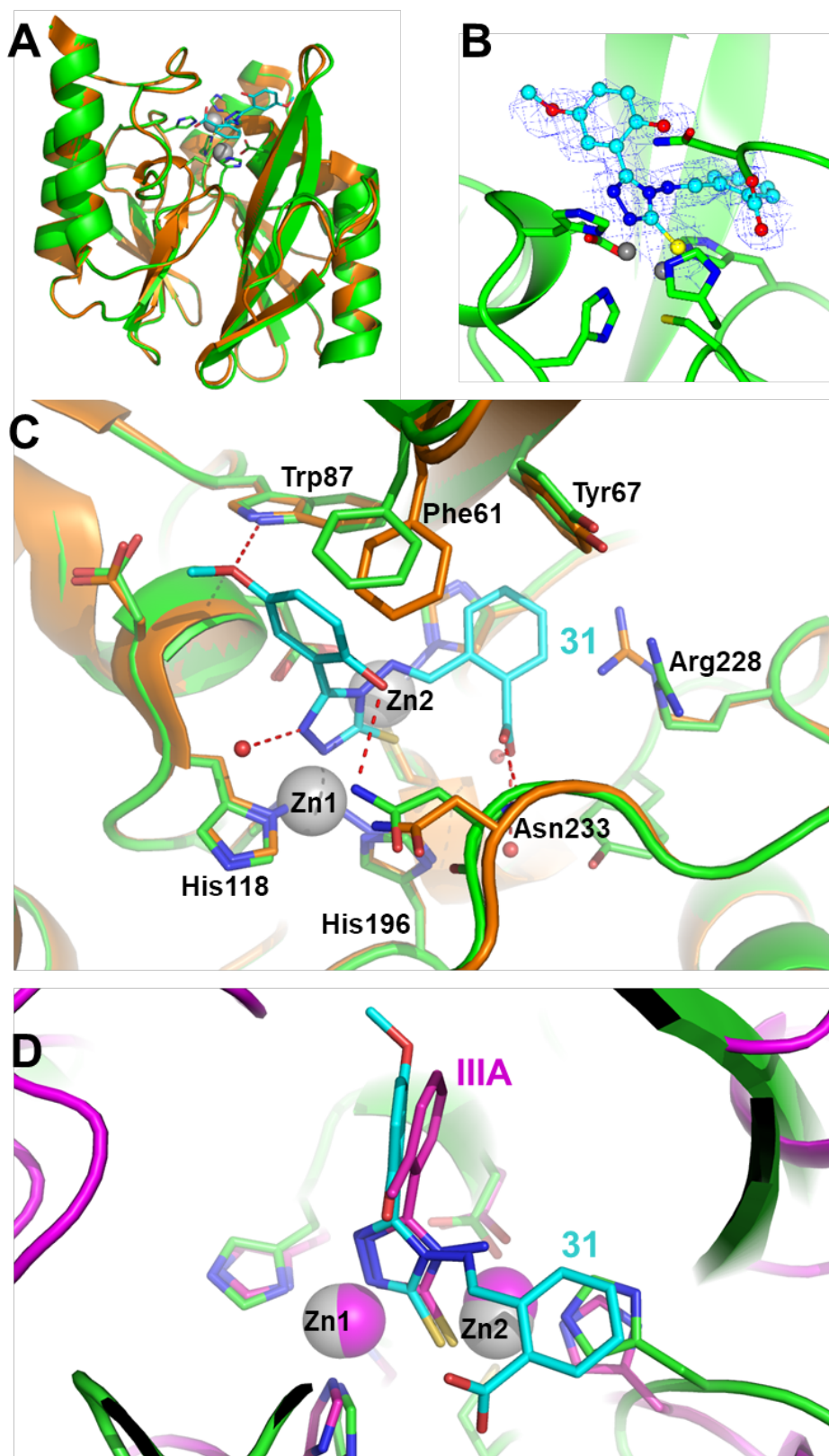


Figure 4. (A) Overall fold of VIM-2 in native form (PDB code, 1KO3; orange) and in complex with compound **31** (JMV4690) (PDB code, 6YRP; green); (B) Close up of the active site region of the VIM-2:**31** complex (the omit map is shown in blue and contoured at approx. 2.5σ); (C) Mode of binding and interactions of **31** with VIM-2 active site residues (green; native VIM-2 is shown in orange; see text for details); (D) Superimposition of the L1:IIIA (PDB code, 2HB9) and VIM-2:**31** complexes, showing the similar positioning of the inhibitor in the dinuclear catalytic site.

3. Conclusions

In conclusion, by varying the two substituents of compound XIII (**1**) at positions 4 and/or 5, we were able to obtain highly potent inhibitors of all tested MBLs. Compared to XIII, individual increases in potency were approximately 400-, 40-, 23-, 85-, 580- and 120-fold against L1 (**43**), VIM-4 (**39**), VIM-2 (**63**), NDM-1 (**40**), IMP-1 (**54** and **66**) and CphA (**87**), respectively. In addition, several compounds showed broad-spectrum inhibition with K_i values in the submicromolar or low micromolar range toward five out of six representative MBLs, including two most clinically relevant enzymes such as VIM-2 and NDM-1. The most interesting inhibitors contained an *o*-benzoic group at the 4-position and a biaryl moiety at the 5-position (**35**, naphth-2-yl; **39**, *m*-biphenyl; **44**, naphth-2-yl-methyl).

Twenty-seven different aryl groups attached at the 5-position of the triazole ring were evaluated (see Table 2). The vast majority (i.e. 22) allowed potent inhibition of at least one MBL and half of these afforded broad-spectrum inhibitors ($K_i < 10.0 \mu\text{M}$ for ≥ 3 MBLs). Twenty-one different aryl groups were evaluated at the 4-position of the triazole ring (see Table 1). In this case, a lower tolerance was observed (only two compounds with $K_i < 10.0 \mu\text{M}$ for ≥ 3 MBLs). In fact, higher potencies were generally measured for compounds with an *o*-benzoic moiety. In particular, VIM-2 was more sensitive to various substitution at this position than other enzymes, whereas VIM-4 and NDM-1 were able to accommodate a larger variety of analogues. IMP-1 showed a clear preference for the *p*-benzyloxyphenyl substituent, that was not at all tolerated by VIM-2, highlighting the substantial structural heterogeneity between the active sites of these two MBLs. Thus, the 4-position appeared a determining factor for selectivity. ITC experiments also highlighted a different binding behaviour between *o*-benzoic-containing compounds and others. The former displayed a favourable entropic contribution for binding while the later displayed the highest enthalpy values.

X-ray crystallography confirmed the original binding mode of triazole-thione with the dinuclear site of MBLs and provided a structural basis for the potent inhibition of VIM-2 by **31**, with the establishment of a network of interactions with relevant residues, such as the conserved Asn233. It also showed the surprising lack of interaction of the inhibitor carboxylate with Arg228, which could be exploited for the design of further inhibitors.

Cytotoxicity experiments and the study of a potential off-target (i.e. glyoxalase II) afforded quite favourable results. Microbiological assays identified several compounds able to potentiate the activity of a β -lactam antibiotic when tested on several MBL-producing laboratory strains,

although there was a lack of correlation between their *in vitro* activity and inhibition potency. Some inhibitors clearly showed a modest ability to accumulate in the periplasm at significant concentrations, because of either active efflux or limited diffusion through the outer membrane. However, we showed that at least one potent NDM-1 inhibitor (**76**) was able to potentiate the activity of carbapenems, and that this potentiation was further improved in the presence of colistin, a polymyxin known for its permeabilizing properties. This supports that additional efforts are worth pursuing to improve the penetration and accumulation in the bacterial periplasm of 1,2,4-triazole-3-thione-based MBL inhibitors. We are now following various strategies known to have an impact on penetration, besides working on expanding the scaffold's chemical space to generate useful SAR data allowing a better understanding of the requirements compatible with a better accumulation of the inhibitor in the periplasm. For instance, potential modifications could address the presence of a negative charge in our most potent compounds potentially deleterious because of the negatively charged lipopolysaccharides of the outer membrane by introducing a positively charged group. Another possibility would be the introduction of a siderophore group to exploit the bacterial metal ion transport system, although the introduction of such group might be less straightforward and more likely to have an impact on the inhibition potency.

Furthermore, one potential weakness of Schiff base analogues is their susceptibility to hydrolysis, which would decrease compound concentration while affording the moderately potent "short" analogues. Although this hydrazone-like bond is quite stable in aqueous solution, it might not be the case in biological media. In support, L1 is suspected to cleave XIII into IIIA. Therefore, we are now focusing on the synthesis of stable analogues either by reduction of the double bond or by its substitution with a stable spacer.

4. Experiment section

4.1. Chemistry section

4.1.1. General methods

NMR. ^1H NMR and ^{13}C NMR spectra were recorded at room temperature on a 300, 400 or 500 MHz instrument in $[\text{D}_6]\text{DMSO}$ solutions (unless otherwise indicated). Chemical shifts are reported in parts per million (ppm) relative to residual solvent signals (DMSO: 2.50 ppm for ^1H and 39.52 for ^{13}C). Splitting patterns in ^1H NMR spectra were designated as follows: s, singlet; d, doublet; t, triplet; q, quartet; m, multiplet; br, broad. **IR spectra** were collected on a Perkin Elmer Spectrum One apparatus. **Mp.** Melting points were determined on a capillary

melting point apparatus. **TLC.** Thin-layer chromatographies were performed on aluminium-backed sheets of silica gel F₂₅₄ (0.2 mm), which were visualized under 254 nm light, and by spraying with a 2% ninhydrin solution in ethanol followed by heating, or by charring with an aqueous solution of ammonium sulphate and sulfuric acid (200 g (NH₄)₂SO₄ and 40 mL concentrated sulfuric acid in 1 L of water). **Analytical reverse phase HPLC.** Samples were prepared in an acetonitrile/water (50/50 v/v) mixture. Compounds insoluble in this mixture were solubilized in DMSO. RP HPLC analyses were performed on a Chromolith SpeedRod C18 column (0.46 x 5 cm) by means of a linear gradient (0-100%) of 0.1% TFA/acetonitrile in 0.1% aqueous TFA over 5 min, and at a flow rate of 3 mL/min. **LC-MS.** The LC/MS system consisted of a Waters Alliance 2690 HPLC, coupled to a Waters Micromass ZQ spectrometer (electrospray ionization mode, ESI+). All analyses were carried out using a RP C18 monolithic Onyx Phenomenex 2.5 x 0.46 cm column. The flow rate was set to 3 mL/min with eluent A (water/0.1% formic acid) and a gradient of 0% →100% of eluent B (acetonitrile / 0.1% formic acid) over 3 min was then used. Positive ion electrospray mass spectra were acquired at a solvent flow rate of 100–500 µL/min. Nitrogen was used as both the nebulizing and drying gas. The data were obtained in a scan mode in 0.1s intervals; 10 scans were added up to get the final spectrum. **HR-MS** were registered on a JEOL JMS-SX-102A mass spectrometer. **Purification.** (i) Column chromatography was performed using Merck silica gel 60 of particle size 40-63 mm. (ii) Reverse phase preparative HPLC purification of some final compounds was performed on a Waters Delta Pak C18 column (40 x 100 mm, 15 µm, 100 angstrom) by means of a linear gradient of eluent B in A at a 1%/min rate (flow rate: 28 mL/min). Eluent A: water; eluent B: acetonitrile. TFA was avoided because of susceptibility of the hydrazone-like bond to acid-promoted hydrolysis during freeze-drying.

The purity of all compounds was determined to be ≥95% by ¹H NMR and reverse phase HPLC.

The preparation of 4-amino-5-substituted-triazole-3-thiones was performed as already reported [28] and is briefly described in Supplementary Information.

4.1.2. General procedure for the preparation of Schiff bases

To a solution of 4-amino-1,2,4-triazole-3-thione (0.5 mmol, 1 eq.) in acetic acid (4 mL) was added a variously substituted arylaldehyde (0.75 mmol, 1.5 eq.). The mixture was heated to reflux for 2h, and then allowed to cool to room temperature. The precipitate was filtered-off and recrystallized in ethanol to provide the corresponding Schiff base.

4.2. Biology section

4.2.1. Metallo- β -Lactamase inhibition assays

4.2.1.1. VIM-type enzymes, NDM-1 and IMP-1

The inhibition potency of the compounds has been assessed with a reporter substrate method and specifically by measuring the rate of hydrolysis of the reporter substrate (150 μ M imipenem for VIM-2, VIM-4, IMP-1; 120 μ M cefotaxime or 100 μ M nitrocefin for NDM-1) at 30 °C in 50 mM HEPES buffer (pH 7.5) in the absence and presence of several concentrations of the inhibitor (final concentration, 0.5–1,000 μ M).

The reaction rate was measured as the variation of absorbance observed upon substrate hydrolysis in a UV-Vis spectrophotometer or microplate reader at a wavelength of 300 nm (imipenem, meropenem), 260 nm (cefotaxime), or 482 nm (nitrocefin) and in the presence of a purified MBL enzyme (such as VIM-2, VIM-4, NDM-1, and IMP-1, at a final concentration ranging from 1-70 nM).

These enzymes were overproduced in derivatives of *E. coli* BL21(DE3) carrying a pET-9a (IMP-1, VIM-2, VIM-4) or pET-15b (NDM-1) vector in which the metallo- β -lactamase-encoding open reading frame was cloned. Bacterial strains were grown in the auto-inducing medium ZYP-5052 supplemented with 50 μ g/ml kanamycin for 24 h at 37 °C [37]. The IMP-1, VIM-2 and VIM-4 were purified by ion-exchange and gel filtration chromatography using an AKTA Purifier platform (GE Healthcare, Uppsala, Sweden) as previously described [38]. NDM-1 was purified using affinity chromatography. After growth for 26 h at 25 °C, bacterial cells were harvested by centrifugation (10,000 \times g, 30 min, 4 °C), resuspended in 10 mM HEPES buffer (pH, 7.5) containing 0.15 M NaCl (buffer A) in one fifth of the original culture volume and lysed by sonication. Cellular debris was removed by centrifugation (12,000 \times g, 40 min, 4 °C). The clarified sample was loaded on a HisTrap HP column (bed volume, 5 ml; GE Healthcare), followed by a wash step (25 ml) with buffer A containing 20 mM imidazole. Proteins were eluted using buffer A containing 350 mM imidazole. The resulting protein sample was desalted (HiPrep 26/10 Desalting column, GE Healthcare) using 20 mM triethanolamine (pH, 7.2) supplemented with 50 μ M ZnSO₄ and concentrated using an Amicon Ultra-15 (MW cut-off, 10 kDa; Millipore, Burlington, Mass.). The concentrated sample was loaded on a Superdex 75 prep grade column (XK16/100 column; bed volume, 140 ml; GE Healthcare) and the proteins eluted with buffer A containing 50 μ M ZnSO₄. The active fractions were pooled and stored at -20 °C. The purity of the protein preparations was estimated >95% by SDS-PAGE

analysis. The authenticity of the enzyme preparations was confirmed by electron spray ionization mass spectrometry, as previously described [39].

The inhibition constants (K_i) were determined on the basis of a model of competitive inhibition by analysing the dependence of the ratio v_0/v_i (v_0 , hydrolysis velocity in the absence of inhibitor; v_i , hydrolysis velocity in the presence of inhibitor) as a function of $[I]$ as already described [40]. The slope of the plot of v_0/v_i vs $[I]$, which corresponds to $K_m^S/(K_m^S + [S])K_i$ (where K_m^S is the K_m value of the reporter substrate and $[S]$ its concentration in the reaction mixture) and allowed the calculation of the K_i value. Alternatively, a Dixon plot analysis was carried out by measuring the initial hydrolysis rates in the presence of variable concentrations of inhibitor and substrate. This allowed K_i values to be determined and supported the hypothesis that the various compounds behaved as competitive inhibitors of the various tested enzymes. The assays were performed in triplicate. Errors were less than 15%.

4.2.1.2. *CphA and L1*

Compounds were prepared as 10 mM solutions in DMSO before dilution with a 15 mM Cacodylate pH 6.5 buffer for CphA and 25 mM HEPES pH 7.5 for L1. L1 and CphA, purified as previously described [27,41,42], were respectively tested with and without 50 μ M final $ZnCl_2$ concentration. The enzymes were used at fixed concentrations between 0.2 and 0.8 nM. The enzyme and the inhibitor (100 μ M) were pre-incubated for 30 min in a volume of 495 μ L at 21°C. Then, for CphA 5 μ L of 10 mM imipenem substrate were added and its hydrolysis was monitored by following the absorbance variation at 300 nm using a Specord 50 PLUS spectrophotometer (Analytik Jena, Germany). For L1, the reporter substrate was nitrocefin (100 μ M final concentration) and its hydrolysis was followed at 482 nm. Experiments were performed at 30 °C. The activity was tested by measuring the initial rates in three samples without inhibitor, which allowed determining the percentage of residual β -lactamase activity in the presence of inhibitors. When the residual activity in the presence of 100 μ M inhibitor was < 30%, the initial rate conditions were used to study the inhibition in the presence of increasing concentrations of compounds (from 1 to 100 μ M) and to determine the competitive inhibition constant, K_i . The Hanes linearization of the Henri-Michaelis equation. was used and K_i was calculated on the basis of the following equation: $v = V_{max}S/[S + K_m(1 + I/K_i)]$ [18]. The assays were performed in triplicate. Errors were less than 10%.

4.2.2. *Microbiological assays*

The potential synergistic activity of selected compounds was assessed by both agar disk-diffusion and broth microdilution methods, according to the CLSI (Clinical Laboratory Standard Institute) recommendations, using Mueller-Hinton broth [43].

In the former, antibiotic-containing disks (30 µg cefoxitin, 10 µg ampicillin or 30 µg ceftazidime) were supplemented with variable amounts, according to both solubility and availability, of the inhibitor (dissolved in DMSO, a maximum volume of 15 µL was deposited on a disk). After incubation (18 hours, 35 ± 1 °C), the diameter of the growth inhibition zone was measured and compared to that obtained in the absence of inhibitor. DMSO and EDTA (220 µg) were used as negative and positive inhibition controls, respectively. Experiments were performed in triplicate.

These tests were performed on MBL-producing isogenic laboratory strains obtained after transforming *Escherichia coli* XL-1Blue (Invitrogen, Carlsbad, USA) and LZ2310 strains with a derivative of the high copy number plasmid pLB-II carrying the cloned *bla*_{VIM-2}, *bla*_{VIM-4}, *bla*_{NDM-1} and *bla*_{IMP-1} genes. Strain LZ2310 is a triple knock-out mutant derived from K12 in which the genes encoding for components of the three major efflux pumps systems were inactivated (genotype, *ΔnorE ΔmdfA N43 acrAI*) [44] and was used to generate an hyperpermeable background for MBL production and investigate the potential contribution of such mechanisms to inhibitor efflux.

The minimum inhibitory concentrations (MICs) of imipenem (IPM), meropenem (MEM), ceftazidime (CAZ) and the combination CAZ-avibactam were determined in triplicate using Mueller-Hinton broth and a bacterial inoculum of 5 × 10⁴ CFU/well, as recommended by the CLSI [45], in both the absence and presence of a fixed concentration (32 µg/ml) of the inhibitor. A multidrug resistant NDM-1-producing *E. coli* clinical isolate present in our collection (SI-001M) was used. This experiment was also performed in the presence of a sub-inhibitory concentration of colistin (0.12 µg/mL).

4.2.3. Inhibition of human glyoxalase II (*hGloII*)

The recombinant enzyme was produced in *E. coli* and purified as described [46]. For measuring GloII activity, the decrease in absorbance resulting from *S*-D-lactoylglutathione ($\epsilon_{240\text{nm}} = 3.1 \text{ mM}^{-1} \cdot \text{cm}^{-1}$) hydrolysis was measured at 25 °C in 100 mM 4-morpholinopropane sulfonate (MOPS) buffer, pH 7.2 in a total volume of 0.5 mL and with a Thermo Evolution spectrophotometer. *S*-D-lactoylglutathione was obtained from Sigma. Inhibitors were dissolved in DMSO and added to the assay mixture containing buffer and substrate before the reaction

was started with enzyme (5-25 nM hGloII). For each assay, background absorbances induced by the inhibitors were taken into account. All experiments were carried out in duplicate. Results are provided as mean values that differed by less than 15%.

4.2.4 Cell toxicity

4.2.4.1. MTT assay

Cell culture: HUVEC were maintained in culture in 10 cm plates with EGM-2 (endothelial cell growth media) containing 10% fetal calf serum (FCS). After reaching confluence, these cells were detached using trypsin and EDTA. The obtained cell suspension was centrifuged and cells were counted and placed in 96-well culture plates at a density of 3000 cells/100 μ L/well. Cells were allowed to adhere for 24h.

MTT assay: cell viability was assessed using the MTT colorimetric assay. The yellow substrate MTT (3-(4,5-dimethylthiazol-2-yl)-2,5-diphenyltetrazolium bromide) is reduced only by metabolically active viable cells through the action of mitochondrial dehydrogenases resulting in the formation of blue formazan crystals, which do not cross the cell membrane and therefore accumulate within viable cells. Solubilization of the crystals with DMSO afforded a purple solution, which intensity is directly proportional to the number of viable cells.

To evaluate its cytotoxicity, HUVEC in 96-wells plates were treated with compound XIII (**1**) (from a 10 mM stock solution in DMSO) at increasing concentrations, 1, 10, 50 and 100 μ M (control = EGM-2 without serum in the presence of 1% DMSO) after removing the adhesion medium. Treated HUVEC were incubated at 37 °C under 5% CO₂ for 48h. The MTT test was then performed. 100 μ l of MTT solution (previously prepared in DMEM without phenol red) were added to each well. After 4h, cells were observed under a microscope and the MTT solution was removed. After adding 50 μ l of DMSO the absorbance of the resulting solution was measured using a microplate reader (TECAN) at a wavelength of 540 nm.

Average absorbance values (+/- SD) were calculated from two experiments done in triplicate (Figure 3S).

4.2.4.2. Membrane integrity and cell viability assays.

The potential cytotoxic activity of compound **76** was evaluated using the commercially available membrane integrity assay (CytoTox 96® non-radioactive cytotoxicity assay, Promega, Madison, WI, USA). The compound was tested for its ability to induce the lysis of HeLa cells by measuring the release of lactate dehydrogenase (LDH) after incubating the HeLa

cell cultures (20,000 cells/well) for 24h (37 °C, 5% CO₂) in DMEM (Dulbecco's Modified Eagle Medium) supplemented with 10% fetal bovine serum, 4.5 mg/mL glucose and 2 mM L-glutamine in the absence and presence of varying concentrations of the compound (up to 250 μM). Further controls included samples containing the medium only or in which cell lysis was induced by the addition of 9% Triton X-100 (maximum LDH release control). The percentage of cytotoxicity was computed as 100 x (sample LDH release)/(maximum LDH release). The variation of the percentage of cytotoxicity allowed to compute an IC₅₀ value (compound concentration inducing 50% cytotoxicity). In addition, a commercial cell viability assay (RealTime-Glo™ MT Cell Viability Assay, Promega) was used to evaluate potential cytotoxicity effects upon longer incubation times (up to 72 hours). The assay was performed as recommended by the supplier, using the above mentioned conditions, except for cell density (1,500 cells/well).

4.2.5. Isothermal titration calorimetry (ITC) analysis of compound binding to VIM-2

ITC titrations were performed on a MicroCal ITC200 (GE-Malvern) equipped with a 200 μl Hastelloy sample cell and an automated 40 μl glass syringe rotating at 1000 rpm. VIM-2 in 10 mM HEPES-NaOH, 0.15 M NaCl, 50 μM ZnSO₄, pH 7.5 was diluted to the desired concentration with the same buffer and was brought to DMSO concentration identical to that of the injected compound. The tested compounds were solubilized in DMSO at 20 mM concentration and were diluted to 200-400 μM with the enzyme buffer, resulting in a final DMSO concentration of 1-2%.

In a standard experiment, VIM-2 (19 μM) was titrated by one initiating injection (0.5 μl) followed by 19 injections (2 μl) of compounds (200-400 μM) at an interval of 150 s. Dilution heat of compound injections into buffer, at the corresponding DMSO concentration, were subtracted from raw data.

The data so obtained were fitted via the non-linear least squares minimization method to determine binding stoichiometry (n), association constant (K_a), and change in enthalpy of binding (ΔH_b°) using ORIGIN 7 software v.7 (OriginLab). The Gibbs free energy of binding, ΔG_b° , was calculated from K_a ($\Delta G_b^\circ = -RT \ln K_a$) and the entropic term, $T\Delta S_b^\circ$, was derived from the Gibbs-Helmholtz equation using the experimental ΔH_b° value ($\Delta G_b^\circ = \Delta H_b^\circ - T\Delta S_b^\circ$).

4.3. X-ray crystallography section.

The VIM-2 β -lactamase was purified and crystallized using the sitting drop method essentially as previously described [15,40]. Crystals of the native enzymes were soaked for up to 60 min with a 5 mM inhibitor solution in the crystallization buffer, prior to flash-freezing in the presence of ethylene glycol as the cryoprotectant. X-ray diffraction data were collected at the European Radiation Synchrotron Facility (ESRF, Grenoble, France). Data were processed as described elsewhere [47,48] and the structures obtained by molecular replacement using the native structure of the corresponding enzyme (PDB code 1KO3), excluding solvent and other ligands. Refinement was performed with REFMAC5 [49] from the CCP4 suite [50], using an iterative manual rebuilding and modelling of missing atoms in the electron density using COOT [51]. Water molecules were added using the standard procedures implemented in the ARP/wARP suite [52]. Data collection and model refinement statistics are shown in Table 1S. The coordinates and structure factors were deposited in the Protein Data Bank under code 6YRP.

Declaration of competing interest

The authors declare that they have no competing financial interests or personal relationships that could have appeared to influence the work reported in this paper.

Acknowledgements

Part of this work was supported by *Agence Nationale de la Recherche* (ANR-14-CE16-0028-01, including fellowships to L.S. and K.K.), the *Deutsche Forschungsgemeinschaft* (BE1540/15-2 within SPP 1710 to K.B.). We thank Mr Pierre Sanchez for mass spectrometry analyses, Lucia Morbidelli and Vanessa Ritrovato for cytotoxicity studies. Thanks are also due to Prof. Lynn Zechiedrich (Baylor College of Medicine, Houston, USA) for providing the *E. coli* strain LZ2310.

Appendix A. Supplementary data

Supplementary data to this article can be found online at...

References

[1] P. Nordmann, T. Naas, L. Poirel, Global spread of carbapenemase-producing Enterobacteriaceae, *Emerg. Infect. Dis.* 17 (2011) 1791-1798.

- [2] T. R. Walsh, M. A. Toleman, The emergence of pan-resistant Gram-negative pathogens merits a rapid global political response, *J. Antimicrob. Chemother.* 67 (2012) 1-3.
- [3] W. C. Reygaert, An overview of the antimicrobial resistance mechanisms of bacteria, *AIMS Microbiol.* 4 (2018) 482-501.
- [4] A. Cassini, L. D. Högberg, D. Plachouras, A. Quattrocchi, A. Hoxha, G. S. Simonsen, M. Colomb-Cotinat, M. E. Kretzschmar, B. Devleeschauwer, M. Cecchini, D. A. Ouakrim, T. C. Oliveira, M. J. Struelens, C. Suetens, D. L. Monnet, Burden of AMR Collaborative Group. Attributable deaths and disability-adjusted life-years caused by infections with antibiotic-resistant bacteria in the EU and the European Economic Area in 2015: a population-level modelling analysis, *Lancet Infect. Dis.* 19 (2019) 56-66.
- [5] K. Bush, Past and present perspectives on β -lactamases, *Antimicrob. Agents Chemother.* 62 (2018) e01076-18.
- [6] T. Palzkill, Metallo- β -lactamase structure and function, *Ann. N. Y. Acad. Sci.* 1277 (2013) 91-104.
- [7] V. R. Gajamer, A. Bhattacharjee, D. Paul, C. Deshamukhya, A. K. Singh, N. Pradhan, H. K. Tiwari, *Escherichia coli* encoding bla_{NDM-5} associated with community-acquired urinary tract infections with unusual MIC creep-like phenomenon against imipenem, *J. Glob. Antimicrob. Resist.* 14 (2018) 228-232.
- [8] J.-D. Docquier, S. Managani, An update on β -lactamase inhibitor discovery and development, *Drug Resist. Updat.* 36 (2018) 13-29.
- [9] C. J. Burns, D. Daigle, B. Liu, D. McGarry, D. C. Pevear, R. E. Trout, β -Lactamase inhibitors. WO Patent WO 2014/ 089365 A1.
- [10] A. Krajnc, P. A. Lang, T. D. Panduwawala, J. Brem, C. J. Schofield, Will morphing boron-based inhibitors beat the β -lactamases? *Curr. Opin. Chem. Biol.* 50 (2019) 101-110.
- [11] A. Krajnc, J. Brem, P. Hinchliffe, K. Calvopiña, T. D. Panduwawala, P. A. Lang, J. J. A. G. Kamps, J. M. Tyrrell, E. Widlake, B. G. Saward, T. R. Walsh, J. Spencer, C. J. Schofield, Bicyclic boronate VNRX-5133 inhibits metallo- and serine β -lactamases, *J. Med. Chem.* 62 (2019) 8544-8556.
- [12] J. C. Hamrick, J.-D. Docquier, T. Uehara, C. L. Myers, D. A. Six, C. L. Chatwin, K. J. John, S. F. Vernacchio S. M. Cusick R. E. L. Trout, C. Pozzi, F. De Luca, M. Benvenuti S. Mangani, B. Liu, R. W. Jackson, G. Moeck, L. Xerri, C. J. Burns, D. C. Pevear, D. M. Daigle,

VNRX-5133 (Taniborbactam), a broad-spectrum inhibitor of serine- and metallo- β -lactamase, restores activity of cefepime in Enterobacterales and *Pseudomonas aeruginosa*, *Antimicrob. Agents Chemother.* 64 (2020) e01963-19.

[13] B. Liu, R. E. L. Trout, G. H. Chu, D. McGarry, R. W. Jackson, J. C. Hamrick, D.M. Daigle, S. M. Cusick, C. Pozzi, F. De Luca, M. Benvenuti, S. Mangani, J.-D. Docquier, W. J. Weis, D. C. Pevear, L. Xerri, C. J. Burns, Discovery of Taniborbactam (VNRX-5133): a broad spectrum serine- and metallo- β -lactamase inhibitor for carbapenem-resistant bacterial infections, *J. Med. Chem.* 63 (2020) 2789-2801.

[14] M. Everett, N. Sprynski, A. Coelho, J. Castandet, M. Bayet, J. Bougnon, C. Lozano, D. T. Davies, S. Leiris, M. Zalacain, I. Morrissey, S. Magnet, K. Holden, P. Warn, F. De Luca, J.-D. Docquier, M. Lemonnier, Discovery of a novel metallo- β -lactamase inhibitor that potentiates meropenem activity against carbapenem-resistant Enterobacteriaceae, *Antimicrob. Agents Chemother.* 62 (2018) e00074-18.

[15] S. Leiris, A. Coelho, J. Castandet, M. Bayet, C. Lozano, J. Bougnon, J. Bousquet, M. Everett, M. Lemonnier, N. Sprynski, M. Zalacain, T. D. Pallin, M. C. Cramp, N. Jennings, G. Raphy, M. W. Jones, R. Pattipati, B. Shankar, R. Sivasubrahmanyam, A. K. Soodhagani, R. R. Juventhala, N. Pottabathini, S. Pothukanuri, M. Benvenuti, C. Pozzi, S. Mangani, F. De Luca, G. Cerboni, J.-D. Docquier, D. T. Davies, SAR studies leading to the identification of a novel series of metallo- β -lactamase inhibitors for the treatment of carbapenem-resistant Enterobacteriaceae infections that display efficacy in an animal infection model, *ACS Infect. Dis.* 5 (2019) 131-140.

[16] R. P. McGeary, D. T. Tan, G. Schenk, Progress toward inhibitors of metallo- β -lactamases, *Future Med. Chem.* 9 (2017) 673-691.

[17] B. M. Liénard, G. Garau, L. Horsfall, A. I. Karsisiotis, C. Damblon, P. Lassaux, C. Papamicael, G. C. Roberts M. Galleni, O. Dideberg, J.-M. Frère, C. J. Schofield, Structural basis for the broad-spectrum inhibition of metallo- β -lactamases by thiols, *Org. Biomol. Chem.* 6 (2008) 2282-2294.

[18] P. Lassaux, M. Hamel, M. Gulea, H. Delbrück, P. S. Mercuri, L. Horsfall, D. Dehareng, M. Kupper, J.-M. Frère, K. Hoffmann, M. Galleni, C. Bebrone, Mercaptophosphate compounds as broad-spectrum inhibitors of the metallo- β -lactamases, *J. Med. Chem.* 53 (2010) 4862-4876.

- [19] J. H. Toney, G. G. Hammond, P. M. Fitzgerald, N. Sharma, J. M. Balkovec, G. P. Rouen, S. H. Olson, M. L. Hammond, M. L. Greenlee, Y. D. Gao, Succinic acids as potent inhibitors of plasmid-borne IMP-1 metallo- β -lactamase, *J. Biol. Chem.* 276 (2001) 31913-31918.
- [20] A. M. King, S. A. Reid-Yu, W. Wang, D. T. King, G. De Pascale, N. C. Strynadka, T. R. Walsh, B. K. Coombes, G. D. Wright, Aspergillomarasmine A overcomes metallo- β -lactamase antibiotic resistance, *Nature*, 510 (2014) 503-506.
- [21] A. Bergstrom, A. Katko, Z. Adkins, J. Hill, Z. Cheng, M. Burnett, H. Yang, M. Aitha, M. R. Mehaffey, J. S. Brodbelt, K. H. Tehrani, N. I. Martin, R. A. Bonomo, R. C. Page, D. L. Tierney, W. Fast, G. D. Wright, M. W. Crowder, Probing the interaction of aspergillomarasmine A with metallo- β -lactamase NDM-1, VIM-2, and IMP-7, *ACS Infect. Dis.* 4 (2018) 135-145.
- [22] A. Matsuura, H. Okumura, R. Asakura, N. Ashizawa, M. Takahashi, F. Kobayashi, N. Ashikawa, K. Arai, Pharmacological profiles of aspergillomarasmimes as endothelin converting enzyme inhibitors, *Jpn J. Pharmacol.* 63 (1993) 187-193.
- [23] O. Samuelsen, O. A. H. Astrand, C. Fröhlich, A. Heikal, S. Skagseth, T. J. O. Carlsen, H. S. Leiros, A. Bayer, C. Schnaars, G. Kildahl-Andersen, S. Lauksund, S. Finke, S. Huber, T. Gjoen, A. M. S. Andresen, O. A. Okstad, P. Rongved, ZN148 – a modular synthetic metallo- β -lactamase inhibitor reverses carbapenem-resistance in Gram-negative pathogens *in vivo*, *Antimicrob. Agents Chemother.* (2020) doi: 10.1128/AAC.02415-19.
- [24] J. Brem, R. Cain, S. Cahill, M. A. McDonough, I. J. Clifton, J. C. Jiménez-Castellanos, M. B. Avison, J. Spencer, C. W. Fishwick, C. J. Schofield, Structural basis of metallo- β -lactamase, serine- β -lactamase and penicillin-binding protein inhibition by cyclic boronates, *Nat. Commun.* 7 (2016) 12406.
- [25] S. J. Hecker, K. R. Reddy, O. Lomovskaya, D. C. Griffith, D. Rubio-Aparicio, K. Nelson, R. Tsivkovski, D. Sun, M. Sabet, Z. Tarazi, J. Parkinson, M. Totrov, S. H. Boyer, T. W. Glinka, O. A. Pemberton, Y. Chen, M. N. Dudley, Discovery of cyclic boronic acid QPX7728, an ultra-broad-spectrum inhibitor of serine and metallo- β -lactamases, *J. Med. Chem.* (2020) doi: 10.1201/acs.jmedchem.9b01976.
- [26] L. Olsen, S. Jost, H. W. Adolph, I. Pettersson, L. Hemmingsen, F. S. Jørgensen, New leads of metallo- β -lactamase inhibitors from structure-based pharmacophore design, *Bioorg. Med. Chem.* 14 (2006) 2627-2635.

- [27] L. Nauton, R. Kahn, G. Garau, J.-F. Hernandez, O. Dideberg, Structural insights into the design of inhibitors of the L1 metallo- β -lactamase from *Stenotrophomonas maltophilia*, *J. Mol. Biol.* 375 (2008) 257-269.
- [28] L. Seville, L. Gavara, C. Bebrone, F. De Luca, L. Nauton, M. Achard, P. Mercuri, S. Tanfoni, L. Borgianni, C. Guyon, P. Lonjon, G. Turan-Zitouni, J. Dzieciolowski, K. Becker, L. Bénard, C. Condon, L. Maillard, J. Martinez, J.-M. Frère, O. Dideberg, M. Galleni, J.-D. Docquier, J.-F. Hernandez, 1,2,4-Triazole-3-thione compounds as inhibitors of dizinc metallo- β -lactamase, *ChemMedChem* 12 (2017) 972-985.
- [29] K. Kwapien, M. Damergi, S. Nader, L. El Khoury, Z. Hobaika, R. G. Maroun, J.-P. Piquemal, L. Gavara, D. Berthomieu, J.-F. Hernandez, N. Gresh, Calibration of 1,2,4-triazole-3-thione, an original Zn-binding group of metallo- β -lactamase inhibitors. Validation of a polarizable MM/MD potential by quantum chemistry, *J. Phys. Chem. B* 121 (2017) 6295-6312.
- [30] P. Vella, W. M. Hussein, E. W. Leung, D. Clayton, D. L. Ollis, N. Mitić, G. Schenk, R. P. McGeary, The identification of new metallo- β -lactamase inhibitor leads from fragment-based screening, *Bioorg. Med. Chem. Lett.* 21 (2011) 3282-3285.
- [31] T. Christopeit, T. J. Carlsen, R. Helland, H. K. Leiros, Discovery of novel inhibitor scaffolds against the metallo- β -lactamase VIM-2 by surface plasmon resonance (SPR) based fragment screening, *J. Med Chem.* 58 (2015) 8671-8682.
- [32] F. Spyraakis, G. Celenza, F. Marcoccia, M. Santucci, S. Cross, P. Bellio, L. Cendron, M. Perilli, D. Tondi, Structure-based virtual screening for the discovery of novel inhibitors of New Delhi Metallo- β -lactamase-1, *ACS Med. Chem. Lett.* 9 (2018) 45-50.
- [33] E. Freire, Do enthalpy and entropy distinguish first class from best in class? *Drug Discov. Today* 13 (2008) 869-874.
- [34] J. E. Ladbury, Calorimetry as a tool for understanding biomolecular interactions and an aid to drug design, *Biochem. Soc. Trans.* 38 (2010) 888-893.
- [35] L. Borgianni, J. Vandenameele, A. Matagne, L. Bini, R. Bonomo, J.-M. Frère, G. M. Rossolini, J.-D. Docquier, Mutational analysis of VIM-2 reveals an essential determinant for metallo- β -lactamase stability and folding, *Antimicrob. Agents Chemother.* 54 (2010) 3197-3204.

- [36] C. Mugnaini, F. Sannio, A. Brizzi, R. Del Prete, T. Simone, T. Ferraro, F. De Luca, F. Corelli, J.-D. Docquier, Screen of unfocused libraries identifies compounds with direct or synergistic antibacterial activity, *ACS Med. Chem. Lett.* 11 (2020) 899-905.
- [37] F. M. Studier, Protein production by auto-induction in high density shaking cultures, *Protein Expr. Purif.* 41 (2005) 207-234.
- [38] N. Laraki, N. Franceschini, G. M. Rossolini, P. Santucci, C. Meunier, E. de Pauw, G. Amicosante, J.-M. Frère, M. Galleni, Biochemical characterization of the *Pseudomonas aeruginosa* 101/1477 metallo- β -lactamase IMP-1 produced by *Escherichia coli*, *Antimicrob. Agents Chemother.* 43 (1999) 902-906.
- [39] J.-D. Docquier, F. Pantanella, F. Giuliani, M. C. Thaller, G. Amicosante, M. Galleni, J.-M. Frère, K. Bush, G. M. Rossolini, CAU-1, a subclass B3 metallo- β -lactamase of low substrate affinity encoded by an ortholog present in the *Caulobacter crescentus* chromosome, *Antimicrob. Agents Chemother.* 46 (2002) 1823-1830.
- [40] J.-D. Docquier, J. Lamotte-Brasseur, M. Galleni, G. Amicosante, J. M. Frère, G. M. Rossolini, On functional and structural heterogeneity of VIM-type metallo- β -lactamases, *J. Antimicrob. Chemother.* 51 (2003) 257-266.
- [41] M. Hernandez-Villadares, M. Galleni, J.-M. Frère, A. Felici, M. Perilli, N. Franceschini, G. M. Rossolini, A. Oratore, G. Amicosante, Overproduction and purification of the *Aeromonas hydrophila* CphA metallo- β -lactamase expressed in *Escherichia coli*, *Microb. Drug Resist.* 2 (1996) 253-256.
- [42] C. Bebrone, C. Anne, K. De Vriendt, B. Devreese, G. M. Rossolini, J. Van Beeumen, J.-M. Frère, M. Galleni, Dramatic broadening of the substrate profile of the *Aeromonas hydrophila* CphA metallo- β -lactamase by site-directed mutagenesis, *J. Biol. Chem.* 280 (2005) 28195-28202.
- [43] Clinical Laboratory Standard Institute, Performance standards for antimicrobial disk susceptibility tests; approved standard, Document M02-A12, 2015, Twelfth Edition, Wayne, PA, USA.
- [44] S. Yang, S. R. Clayton, E. L. Zechiedrich, Relative contributions of the AcrAB, MdfA and NorE efflux pumps to quinolone resistance in *Escherichia coli*, *J. Antimicrob. Chemother.* 51 (2003) 545-556.

- [45] Clinical Laboratory Standard Institute, Methods for dilution antimicrobial susceptibility tests for bacteria that grow aerobically, Document M07-A10, 2015, Twelfth Edition, Wayne, PA, USA.
- [46] M. Akoachere, R. Iozef, S. Rahlfs, M. Deponce, B. Mannervik, D. J. Creighton, H. Schirmer, K. Becker, Characterization of the glyoxalases of the malarial parasite *Plasmodium falciparum* and comparison with their human counterparts, *Biol. Chem.* 386 (2005) 41-52.
- [47] J.-D. Docquier, M. Benvenuti, V. Calderone, M. Stoczko, N. Menciassi, G. M. Rossolini, S. Mangani, High-resolution crystal structure of the subclass B3 metallo- β -lactamase BJP-1: rational basis for substrate specificity and interaction with sulfonamides, *Antimicrob. Agents Chemother.* 54 (2010) 4343-4351.
- [48] C. Pozzi, F. Di Pisa, F. De Luca, M. Benvenuti, J.-D. Docquier, S. Mangani, Atomic-resolution structure of a class C β -lactamase and its complex with avibactam, *ChemMedChem* 13 (2018) 1437-1446.
- [49] G. N. Murshudov, P. Shubak, A. A. Lebedev, N. S. Pannu, R. A. Steiner, R. A. Nicholls, M. D. Winn, F. Long, A. A. Vagin, REFMAC5 for the refinement of macromolecular crystal structures, *Acta Crystallogr. D Biol. Crystallogr.* 67(Pt4) (2011) 355-367.
- [50] M. D. Wynn, C. C. Ballard, K. D. Cowtan, E. J. Dodson, P. Emsley, P. R. Evans, R. M. Keegan, E. B. Krissinel, A. G. Leslie, A. McCoy, S. J. McNicholas, G. N. Murshudov, N. S. Pannu, E. A. Potterton, H. R. Powell, R. J. Read, A. Vagin, K. S. Wilson, Overview of the CCP4 suite and current developments, *Acta Crystallogr. D Biol. Crystallogr.* 67(Pt4) (2011) 235-242.
- [51] P. Emsley, B. Lohkamp, W. G. Scott, K. Cowtan, Features and development of Coot, *Acta Crystallogr. D Biol. Crystallogr.* 66(Pt4) (2010) 486-501.
- [52] G. Langer, S. X. Cohen, V. S. Lamzin, A. Perrakis, Automated macromolecular model building for X-ray crystallography using ARP/wARP version 7, *Nat. Protoc.* 3 (2008) 1171-1179.